Archiv-Ex.:

FZR - 36

FZR
FORSCHUNGSZENTRUM ROSSENDORF

Institute of Ion Beam Physics and Materials Research

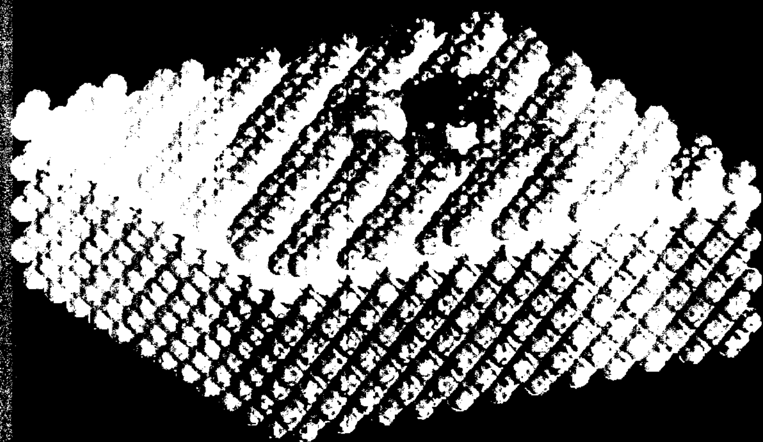

Annual Report 1993

Postfach 510119
D-01314 Dresden, Germany
Tel.: +49-351-591-22 45
Fax: +49-351-591-32 85

FORSCHUNGSZENTRUM ROSSENDORF
INSTITUT FÜR IONENSTRAHLPHYSIK UND MATERIALFORSCHUNG

Annual Report 1993

Editors:
W. Möller, E. Wieser, S. Kirch

FZR36
April 1994

For further information on the research projects described in the present annual report, please address the director or one of the authors at the institute.

Postal address:

Postfach 51 01 19
D-01314 Dresden
Germany

Telecommunication:

Tel.: +49 351 591 2245
Fax: +49 351 591 3285
E-mail moellerw
@fz-rossendorf.de

Contents

Preface 5

Highlights

Ion Beam Induced Epitaxial Crystallization of 6H-SiC 7

Band Gap Engineering in Co Alloyed ß-$FeSi_2$ Formed by Ion Beam Synthesis 9

Formation of $CoSi_2$ Wires by maskless Implantation with the focused Ion Beam 11

Phosphorus Implanted n^+-Layers for High Purity Germanium Detectors 13

Development of a Fluidic ISFET Microsystem for Chemical Analysis 15

Depth Selective Mössbauer Spectroscopy on Al-implanted Iron 17

Plasma Source Ion Implantation 20

Simultaneous Light Element Analysis by HIERD for Plasma-Wall Interaction Studies in Fusion Research 23

Paint Layer Studies using PIXE on Air 26

Texture Investigation on Geological Three Phase Samples 29

Status of the Rossendorf 7.25 GHz ECR Ion Source: Measurement of Electron Energy Distribution and Characteristic X-Ray Spectra 31

Formation of Double-Height Si(001) Steps by Sputtering with Xe Ions - a Computer Simulation 34

Self-Organisation During Ostwald Ripening in Ion Beam Synthesis of Buried Compound Layers 37

Short Contributions

Modification of Metals and Other Materials 40

Modification of Semiconductors and Patterning by Focused Ion Beam 43

Application of Ion Beams to Sensors 47

Ion Beam Analysis, Fundamentals of Ion-Solid-Interaction and Accelerator Technique 51

Structural Research 54

Theory of Ion Beam Induced Processes in Solids 57

Statistics

Publications 60

Conference Contributions 64

Seminars 72

Reports 74

Patents 75

Departments of the Institute 76

List of Personnel 77

Preface

The Research Center Rossendorf has been established at the beginning of 1992 as the successor of the largest nuclear research facility of the former German Democratic Republic. Its institutes are partly pursueing research activities in fields where already the former institution had demonstrated success and high international standard. However, new directions have been established especially in areas with high technological and environmental potential. Future research will focus along two main streams of materials research and biomedicine/chemistry. This requires the installation of new research facilities, but also the completion of basic equipment and the restoration of buildings and infrastructure. In addition, the scientists have to be integrated into the national and international communities with their traditions of communication and publication. Thus, the year 1993 is a part of a transient phase towards a modern and high-standard establishment.

The institute of Ion Beam Physics and Materials Research is devoted to the application of ion beams for the modification and the analysis of near-surface layers of solids. The research activities aim at combining closely basic studies and investigations of technological application. For the modification of materials, a broad range of ion-based techniques is available, such as ion implantation, and ion- and plasma-assisted thin film deposition. Correspondingly, characteristic ion energies being available range from about 10 eV for plasma processes to more than 10 MeV from heavy ion implantation.

Main fields of application are the improvement of mechanical surface properties in particular for light metals, defect engineering and the production of buried layers in semiconductors (in particular silicon carbide), and the preparation of special radiation detectors and ion-sensitive microsensors. Technical process development is accompanied by experiments which improve the understanding of the basic physical and chemical mechanisms. For this purpose, in-situ diagnostics play a prominent role. In connection with the experimental studies, theoretical investigations are being performed, in particular using computer simulation programs.

High-energy ion beam analysis is employed as an important tool for the characterization of near-surface layers, both for the institute's scientific program and for external services. The institute offers a broad range of such methods and is continuously improving the corresponding facilities and data reduction techniques.

Historically, the institute is also involved in neutron diffraction studies, now at external facilities. These activities will be gradually reduced in favour of local X-ray diagnostics.

For the above experimental and theoretical investigations, the institute can rely on a permanent total staff of 80 persons, including 32 professional scientists, and 2 Post Docs. The institute succeeded in recruiting another 23 coworkers in 1993 from different external projects. These are of vital importance as the main source of integrating young scientists. The projects are being sponsored by a wide range of organizations such as the Saxony and the German federal governments, the European Union, and industry. The institute is also very pleased with 13 PhD students, about half of which have been hired from external sources.

Considerable progress was achieved in 1993 in establishing the external relations of the institute and defining its role in regional, national and international programs. By the simultaneous installation of its director as a professor for Ion Beam Physics at the Technical

University of Dresden, it will contribute significantly to teaching and education especially in a field, which hitherto had been little represented at German universities. The institute became a constituting member of the Dresden Materials Research Community, which represents about 300 professional scientists in different organizations at the university, the Max-Planck and Fraunhofer societies, and other research institutions.

In connection with the opening ceremony of the TANDETRON accelerator in December 1993, the institute arranged a meeting on problems of high-energy ion beam analysis with all German experts in the field, who decided to establish continuous communication with regular meetings. The electrostatic accelerators and implanters of the institute were acknowledged as a "large research facility" by the German Federal Minister of Research and Technology, in order to offer ion beams for solid state research within a forthcoming program involving a large number of groups from German universities.

Within the Human Capital and Mobility program of the European Union, the institute has been chosen as a center of excellence where young scientists from other European countries are invited to work on the basis of European grants. Within the same program, the institute takes also part in a "Network" on ion beam processing of semiconductors.

In 1993, the institute succeeded in considerably extending its experimental facilities by purchasing and commissioning a new accelerator and several diagnostic devices. A 3 MV high-current TANDETRON accelerator was installed and set into operation. It will mainly serve for high-fluence, large-depth ion beam modification, but also enable large-depth ion beam analysis. Several ex-situ diagnostic tools became available, such as a Fourier-transform infrared spectrometer, a spectroscopic ellipsometer, and a scanning tunneling/atomic force microscope. Additional laboratory devices were constructed and operated, such as a large-volume IBAD (Ion Beam Assisted Deposition) chamber, and a plasma immersion implantation setup. A laboratory assembling three different annealing furnaces including a reactive gas supply was established.

The experimental activities until February 1993, and, correspondingly, the scientific output throughout the whole year suffered from a temporary shutdown of the the electrostatic accelerators and implanters, due to a missing approval by the technical supervision authorities. Nevertheless, appreciable progress and performance could be demonstrated in a number of fields. The present annual report will first address some of such "highlights" in a more detailed presentation. Subsequently, a complete overview will be given on the results of the research projects of the different departments.

Ion Beam Induced Epitaxial Crystallization of 6H-SiC

V. Heera, R. Kögler, W. Skorupa and E. Glaser*
* FSU Jena, Institute of Solid State Physics, Max-Wien-Platz 1, D-07743 Jena, Germany

SiC is a semiconductor material with promising properties for high temperature applications. Unfortunately, it is very difficult to anneal lattice damage in crystalline SiC or to recrystallize amorphous SiC [1], e.g. solid phase epitaxy (SPE) of SiC needs temperatures above 1450°C. Ion irradiation may be used for low temperature recrystallization of amorphous surface layers in some semiconductors. This ion beam induced epitaxial crystallization (IBIEC) has been extensively investigated in silicon material [1] and was found to occur also in several compounds. It was shown that IBIEC can take place already at temperatures much below the threshold temperature of the thermally induced SPE. For instance, IBIEC of silicon is possible at 150°C, whereas a temperature of 550°C is necessary for thermally induced SPE in this material. Therefore, we have investigated the possibility of IBIEC in SiC below 500°C [3]. Amorphous surface layers of about 140 nm thickness were produced by 200 keV, $5{\cdot}10^{14}$ Ge^{+}/cm^{-2} implantation into single crystalline 6H-SiC wafers from Cree Research Inc.. The wafer was then cut into pieces of about 1 cm^2 and half-capped by Si wafer pieces to preserve unirradiated reference regions. After a surface cleaning procedure the SiC specimens were mounted on a heating stage in the implantation chamber and pre-heated to a temperature of about 400°C. Subsequently the specimens were subjected to 300 keV Si^+ irradiation in the dose range between $1{\cdot}10^{16}cm^{-2}$ and $3{\cdot}10^{17}$ cm^{-2}. The ion flux was about $3{\cdot}10^{12}$ $cm^{-2}s^{-1}$ and led to an additional temperature increase. During the ion irradiation the total temperature was adjusted to 477$\pm$5°C. The amorphous surface layers were analyzed before and after the IBIEC irradiation with 1.2 MeV He^+ RBS/C .

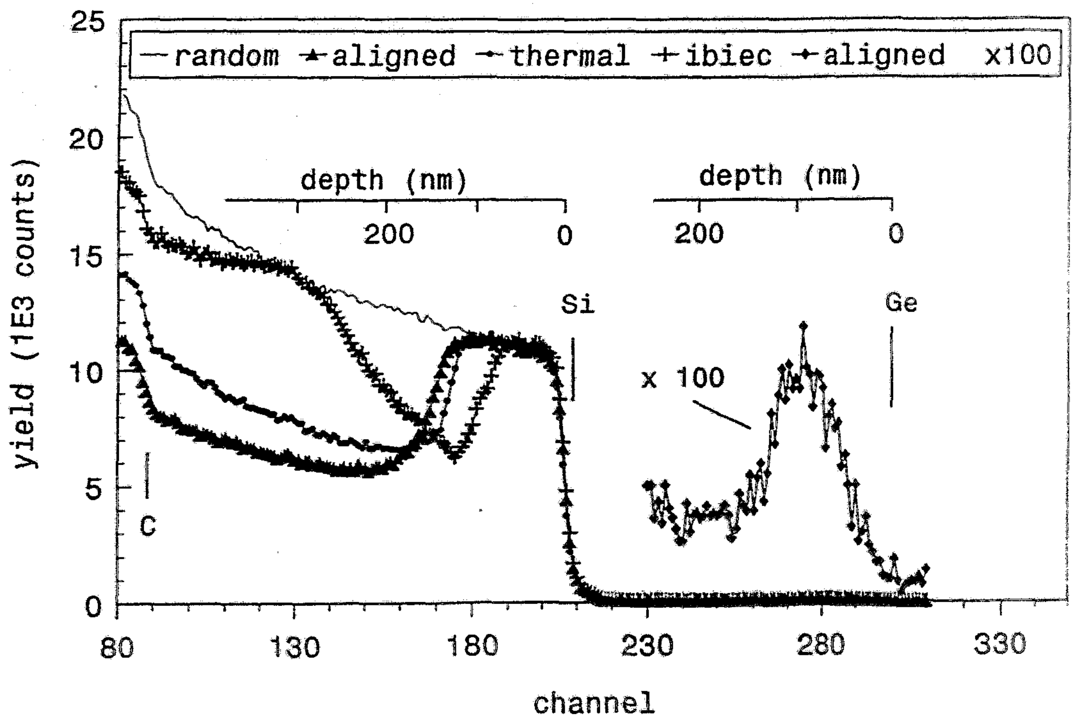

Fig. 1. RBS/C spectra of the amorphous SiC layers. Further explanation see below.

Fig. 1 shows an overview of the RBS/C spectra, which involves the aligned and random spectrum of the as-amorphized state as well as the covered (thermal) and uncovered part (ibiec) of the specimen which was irradiated with the Si^+ ions. The 300 keV Si irradiation at 477°C leads to an obvious shrinkage of the initial amorphous layer thickness. In the case of $3{\cdot}10^{17}$ Si^+cm^{-2} nearly half of the initial amorphous layer is recrystallized. As can be seen in Fig. 1, the dechanneling rate increases substantially in the region behind the amorphous layer. This is caused by the Si irradiation damage. The RBS/C spectrum touches the random level at a depth of about 320 nm, which is in good agreement with the calculated mean projected range of 300 keV Si^+ in SiC.

A small recrystallized layer of about 20 nm has been observed also in the region of the specimen that was covered to remain a reference sample without Si ion irradiation (see RBS/C spectrum denoted as "thermal" in Fig. 1). Obviously, a small part of thermally stimulated SPE takes place already at the temperature of 477°C. However, this process comes to rest after 20 nm and cannot be continued at this temperature without ion irradiation.

The IBIEC process proceeds with increasing ion dose. A total recrystallized layer thickness (thermal and IBIEC part) of 57 nm was obtained for the dose of $3{\cdot}10^{17}cm^{-2}$. In Fig. 2 the IBIEC part of the regrown layer thicknesses (total recrystallized layer thickness minus thermal regrown one) is given in dependence on the ion dose. There is an initial IBIEC rate of about 8 nm/ $10^{16}cm^{-2}$. Only a very small additional regrowth is obtained for $5{\cdot}10^{16}cm^{-2}$. For the ion doses higher than $1{\cdot}10^{16}cm^{-2}$ the mean IBIEC rate amounts to about 1.5 nm/ $10^{16}cm^{-2}$ (dashed line in Fig. 2). This is, compared to IBIEC in Si, a very low recrystallization rate. It should be noted, however, that the temperature at which the IBIEC process in SiC has been observed is about 1000° below the threshold temperature for complete thermal SPE. We believe, that the IBIEC process in SiC is stimulated by point defect migration and, therefore, at higher temperatures higher recrystallization rates can be achieved.

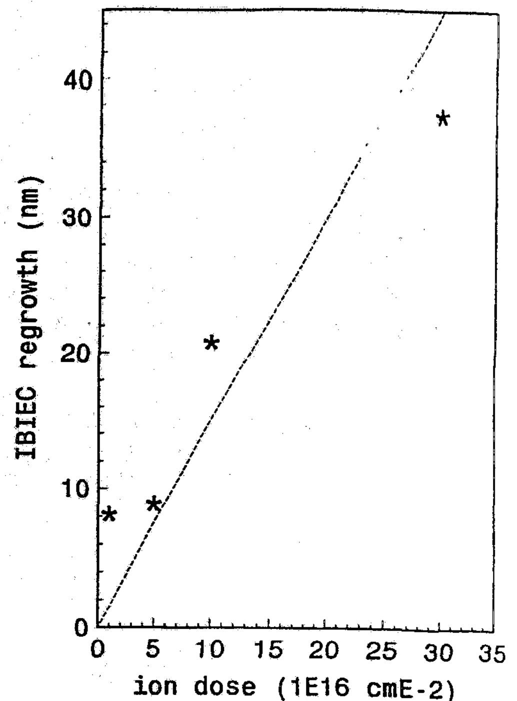

Fig. 2. Layer thickness regrown by IBIEC versus Si^+ ion dose

1. R. F. Davies and J. T. Glass, Advances in Solid State Chemistry 2, (1991) 1.
2. F. Priolo and E. Rimini, Mater. Sci. Rep. 5, (1990) 319.
3. V. Heera, R. Kögler, W. Skorupa and E. Glaser,Mat. Res. Soc. Symp. Proc. 316, (1994) ; in press

Band Gap Engineering in Co Alloyed β-$FeSi_2$ Formed by Ion Beam Synthesis

D. Panknin, W. Henrion*, E. Wieser, M. Voelskow, and W. Skorupa
*Hahn-Meitner-Institut, Berlin

β-$FeSi_2$ is a direct semiconductor with a band gap of about 0.85 eV. This corresponds to a wavelength of 1.45 µm [1] which is near the absorption minimum of silicia optical fibres (about 1.55 µm, = 0.8 eV). Thus, β-$FeSi_2$ should be promising for optoelectronic device applications in the infrared region, integrated in a silicon technology. With regard to this application investigations are of interest to tune the band gap by addition of a third element into $FeSi_2$, for instance cobalt.
In order to synthesize β-$(Fe_{1-x}Co_x)Si_2$ a two step implantation was used. In a first step iron was implanted ($4x10^{17}$ cm^{-2}, 300 keV at 350°C) into (100)-Si wafers. Subsequently, the samples were annealed at 1050°C for 30 min. This results in a buried α-$FeSi_2$ layer containing large crystallites without defects [2]. The following Co implantation (from $3x10^{16}$ cm^{-2} to $9x10^{16}$ cm^{-2}, 300 keV) was carried out at 180°C. The implantation temperature was chosen in order to achieve a partial amorphization of the silicide layer. Subsequent to the Co^+ implantation all samples were annealed isothermally at 750°C in steps of 1 h up to 11 h to transform the α-phase into the semiconducting β-structure. Finally, the samples were annealed at 800°C for 60 min. The temperature of 800°C is an upper limit to retain the β-structure especially for the highest Co concentration [3].
The physical properties of the β-$(Fe_{1-x}Co_x)Si_2$ layers were investigated by Rutherford backscattering spectroscopy (RBS), by cross sectional transmission electron microscopy (XTEM) and infrared spectroscopy (IR).
The atomic concentration ratio Si/metal was calculated from the RBS spectra measured with random incidence and is independent of the assumed silicide density. It should be noted that it is not possible to distinguish between iron and cobalt atoms using RBS. For the β-$FeSi_2$ layer as well as for the samples additionally implanted with Co up to the dose of $6x10^{17}$ Co^+cm^{-2} a concentration ratio Si/metal = 2.1 is determined. A further enhancement of the Co dose causes a small decrease of the ratio to Si/(Fe+Co) = 2.0. This points to a shift of the stoichiometric composition of this ternary silicide [4]. Traces of Co silicide have not been detected by x-ray diffraction also for this high Co admixture [5].
The XTEM investigations show a buried silicide layer containing large crystallites. With increasing Co concentration the width of the silicide layer increases and the size of the silicide crystallites diminishes. For the highest Co concentration, however, relatively large thickness inhomogeneities are observed due to rough interfaces. The Si top layer remains crystalline and contains twin defects. Below the silicide layer a defective layer is found containing mainly dislocation loops [4].
The band gap energy E_g of β-$(Fe_{1-x}Co_x)Si_2$ was determined from IR transmission and reflection measurements using a plot of $(\alpha*d)^2$ versus photon energy (α - absorption coefficient, d - thickness of the silicide layer). In the Fig.1 E_g is shown in dependence on the Co content. With increasing Co concentration the gap decreases from 0.84 eV for pure β-$FeSi_2$ to 0.68 eV for a replacement of 15 % of the iron atoms by cobalt.

With increasing x the absorption of the silicide layer increases both in the edge region of the silicide and towards larger wavelength. This additional absorption mechanism could be caused by an enhanced density of defect related states in the center of the gap [4].

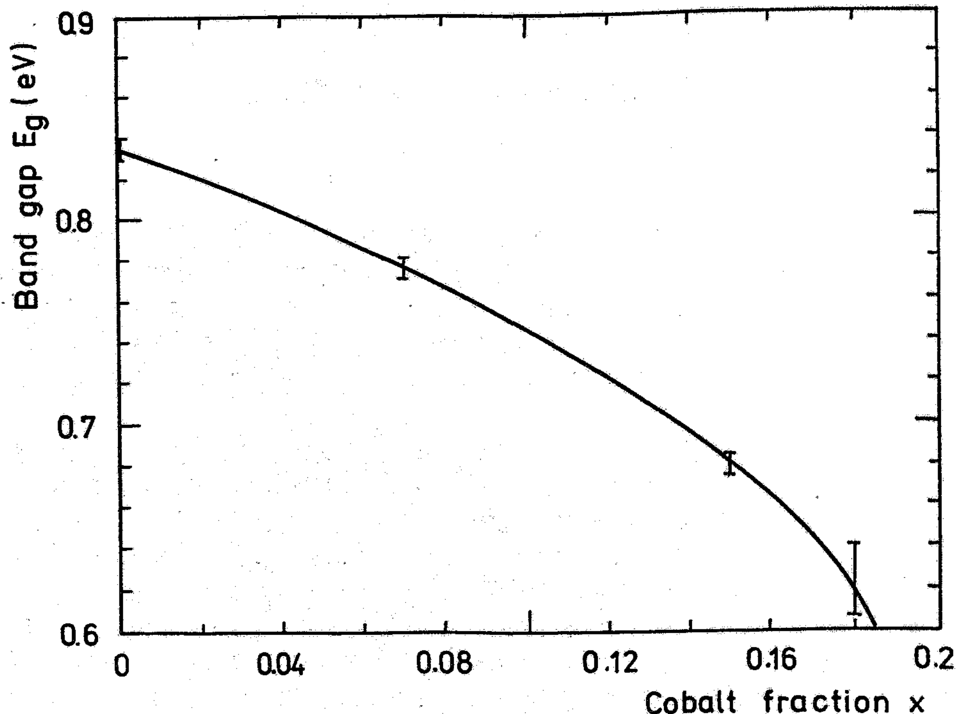

Fig. 1: Band gap energy E_g of the $(Fe_{1-x}Co_x)Si_2$ layer in dependence on the Co content x

The results of this work give the first clear experimental evidence that a distinct change of the band gap energy of β-$FeSi_2$ is possible by ion beam synthesis of $(Fe_{1-x}Co_x)Si_2$. This enables an optimum adjustment of the gap of β-$(Fe_{1-x}Co_x)Si_2$ for special optoelectronic applications in the wavelength region between 1.45 µm and 1.82 µm.
The decrease of the band gap with increasing cobalt content can be explained by the formation of band tail states connected with the increasing carrier concentration. For the highest Co concentration the influence of the lattice distortion on the band structure becomes obviously important as indicated by the non-linear behaviour of the $(\alpha^*d)^2$ plot [4].

[1] K. Lefki, P. Muret, N. Cherief, and R. Cinti, J. appl. Phys. 69 (1991) 352
[2] D. Panknin, E. Wieser, W. Skorupa, G. Querner, H. Vöhse, and J. Albrecht, Mat. Res. Symp. 279 (1993) 111
[3] E. Wieser, D. Panknin, W. Skorupa, G. Querner, W. Henrion, and J. Albrecht, Nucl. Instr. and Methods B 80/81 (1993) 867
[4] D. Panknin, W. Henrion, E. Wieser, M. Voelskow, W. Skorupa, and H. Vöhse, Mat. Res. Soc. Fall Meeting, Boston 1993
[5] D. Panknin, F. Eichhorn, E. Wieser, W. Skorupa, W. Henrion, and J. Albrecht, E-MRS 1993, May 4-7, Strasbourg, to be published in Nucl. Instr. and Methods B

Formation of $CoSi_2$ Wires by maskless Implantation with the focused Ion Beam

J. Teichert, L. Bischoff and E. Hesse

Layers of $CoSi_2$ in Si can be successfully fabricated by high dose cobalt implantation and subsequent annealing. High-quality single crystalline, buried layers may be obtained if the Si substrate is heated during implantation [1]. The formation of continuous $CoSi_2$ layers requires implantation doses higher than a critical dose. The value of the critical dose is determined by the Co peak concentration after implantation which must exceeds half 9 the stoichiometric value (16.7 %) [2]. The layer formation depends sensitively on the implantation temperature [3]. At low temperatures the Si substrate becomes amorphous due to the high-dose Co implantation. Then the Co shifts towards the surface and for low energy implantations $CoSi_2$ precipitates at the surface are obtained. Recently, submicron $CoSi_2$ wires were produced by electron beam patterning of a SiO_2 mask followed by ion beam synthesis [4].

Maskless ion implantation with Focused Ion Beam (FIB) has been developed as a new method for the ion beam synthesis of cobalt silicide wires. The use of FIB implantation raises the possibility of writing directly $CoSi_2$ structures of arbitrary shape in the submicron range. First investigations aimed at reproducing the $CoSi_2$ fabrication technique etablished for broad beam implantation. Investigations of microbeam implantation of Co^+ (30 keV) and Co^{++} (60 keV) with doses between 5×10^{16} and 5×10^{17} ions cm^{-2} into <111> Si were carried out at sample temperatures of RT, 200 °C, 300 °C, and 400 °C. The length of the implanted lines was 200 μm, their width about 2 μm. The ion currents were 1.3 nA (Co^+) and 0.6 nA (Co^{++}), respectively. The samples were annealed (600 °C, 60 min and 1000 °C, 30 min in N_2) after implantation and investigated by SEM and EDX.

The dose rate is different by orders of magnitude comparing implantation experiments performed with the broad beam (e.g. 1.5×10^{13} cm^{-2} s^{-1} in [4]) and our FIB implantation with 2.6×10^{17} cm^{-2} s^{-1} (Co^+) and 6.3×10^{16} cm^{-2} s^{-1} (Co^{++}). The high current density of the FIB implies a very large heat input of about 3 kW/cm^2 into the implanted region. However, an estimation of Melngailis [5] showed that due to the small beam spot and the relatively high heat flow in silicon the temperature rise is negligible. On the other hand so called self-annealing effects in the case of FIB implantation are reported [6]. After p- and n-type FIB doping of GaAs a clear reduction of damage was found compared with that caused by broad beam implantation. In view of these contradictory arguments concerning substrate heating in the FIB implantation case the investigations were started with a RT substrate. For the 30 keV Co^+ as well as the 60 keV Co^{++} implantation formation of $CoSi_2$ at the surface was observed, but the lines appear inhomogeneously as discontinuous films. We found no evidence for 'self-annealing' effects as these results agree well with the ones for broad beam implantion at RT [3], where after implantation with ion energies below 70 keV and subsequent annealing similar $CoSi_2$ surface layers were obtained. The electrical resistivity measurements of the implanted lines show a continuously decreasing resitivity with increasing cobalt dose in the as-implanted state. After the 600 °C annealing a sharp decrease at a critical dose of 7×10^{16} cm^{-2} can be observed caused by the silicide formation. In spite of the imperfection of the $CoSi_2$ film a final resistivity of 162 μΩcm was found. Although this value is higher than that for continuous buried epitaxial layers (13 μΩcm [3]) it is low enough for many applications (e.g. micromechanical devices) [7].

The results of the RT implantation confirm the need for a heated substrate in analogy to the broad beam implantation. The influence of the substrate temperature on the $CoSi_2$ formation is illustrated in Fig. 1. It shows SEM images with high magnification from lines implanted with $3x10^{17}cm^{-2}$ Co^{++} (60 keV) at RT, 200°C, 300°C, and 400 °C after annealing. In the RT case the $CoSi_2$ film (light) is not closed and contains large areas of Si precipitates (dark spots). With increasing implantation temperature the lines appear more and more homogeneous. The image of the 200 °C implantation (Fig. 1b) shows a striking structure like a pearl chain in the center of the line. It may be caused by the fact that the implantation dose is higher in the middle of the line due to the Gaussian current density profile of the beam. The line of the 400 °C implantation looks completely homogeneous. The $CoSi_2$ appears as a closed film without Si precipitates. There are only some small $CoSi_2$ precipitates in the Si near the interface. That observed behaviour agrees well with the substrate temperature dependence of broad beam implantation where continuous buried epitaxial layers were obtained for temperatures above 300 °C [3]. This substrate heating prevents the Si amorphization. It is worthwhile to note that this effect occurs nearly at the same temperature for both implantation types although the FIB dose rate and the resulting damage rate is much higher.

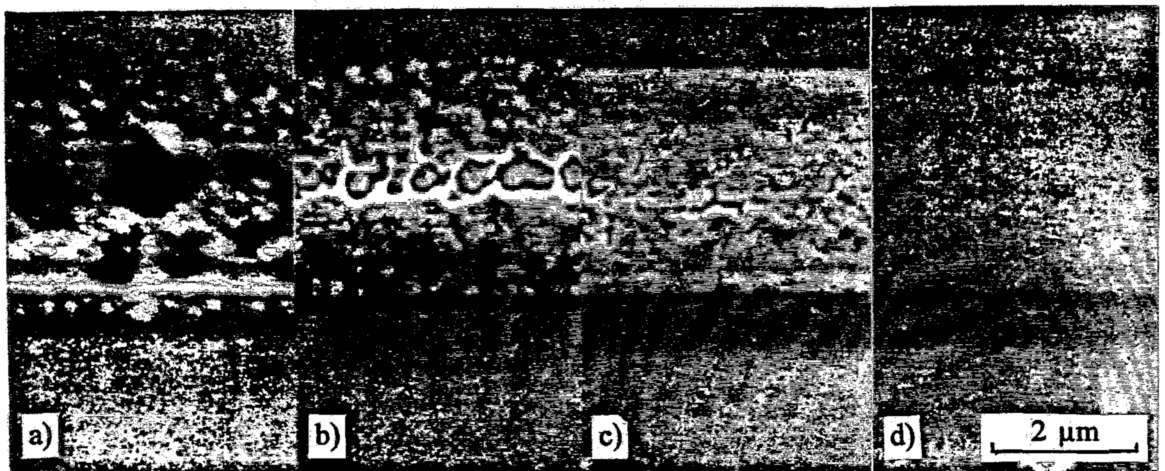

Figure 1. SEM images (top view) of $CoSi_2$ lines (Co^{++}, 60 keV, 3 x 10^{17} cm^{-2}) for different implantation temperatures: a) RT , b) 200°C, c) 300°C, d) 400 °C.

References

1. A.E.White, K.T.Short, R.C.Dynes, J.P.Garno and J.M.Gibson, Appl.Phys.Lett. **50**, 95 (1987).
2. K. Kohlhof, S. Mantl, W. Jäger and B. Stritzker, Appl. Surf. Sci. **38**, 207 (1989).
3. K. Radermacher, S. Mantl, K. Kohlhof and W. Jäger, J. Appl. Phys. **68**, 3001 (1990).
4. N.M. Zimmermann, J.A. Liddle, A.E. White and K.T. Short, Appl. Phys. Lett. **62**, 387 (1993).
5. J. Melngailis, J. Vac. Sci. Technol. **B5**, 469 (1987).
6. Y. Bamba et al., Jap. J. Appl. Phys. **22**, L650 (1983) and **23**, L515 (1984).
7. J. Teichert, L. Bischoff, E. Hesse, D. Panknin and W. Skorupa, MRS Fall Meeting, Boston, USA, Nov. 29 - Dec. 03 , 1993.

Phosphorus Implanted n^+-Layers for High Purity Germanium Detectors

J. von Borany, J. Goerigk and W. Voitus

The present investigations are directed to the development of fully ion implanted, planar HP-Ge-detectors as basic elements for a stack detector system planned for EUROBALL experiments. These detectors have to be frequently annealed due to radiation defects from the neutron component in nuclear reactions. Therefore the usually applied Li- diffused n^+- contact has to be replaced by a temperature stable contact system. Physical problem arises from the strong difference in the annealing behaviour of boron and donor doped layers in germanium. Boron implanted layers show a full electrical activation already after an annealing at 200°C, whereas P^+ and As^+ donor implanted layers have to be annealed and activated above 350°C. Temperatures above 300°C are critical and can change the substrate net doping ($N \sim 10^{10}$ cm^{-3}) as a result of copper and hydrogen induced acceptor states. However, the stability of substrate doping is a strong demand for detectors with several mm depletion depth.

In addition to a careful optimization of furnace annealing, intensive flash lamp pulses are employed for the annealing of phosphorus implanted layers. The application of flash lamps (tp=20 ms) results in a strong temperature gradient realizing the annealing temperature in the implanted surface layer with reduced thermal exposure of the bulk material.

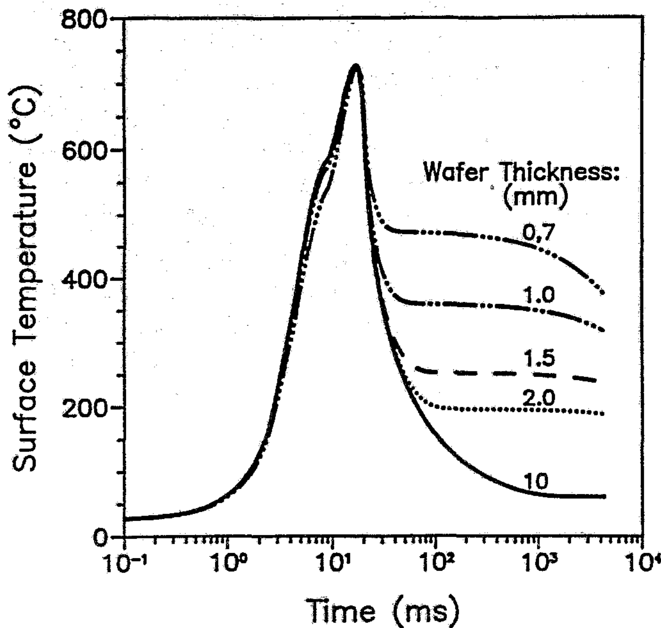

The temperature response was numerically calculated considering the temperature dependence of material properties and process parameters. Fig.1 shows the surface temperature during the annealing cycle for different wafer thicknesses at a maximum surface temperature of 720°C. The maximum bulk temperature for a wafer of several mm thickness is below 300°C, illustrated by the plateau in the curves of Fig.1.

Fig. 1
Calculated surface temperatures versus time during flash lamp annealing for T_{max}= 720°C

The flash lamp annealing has been modified to obtain a different constant substrate temperatures by preheating to T=200°C. Even then, the maximum temperature of detectors of several mm thickness will stay below the critical temperature of 300°C during pulse annealing. The annealing behaviour of the phosphorus implanted layers were determined by the RBS-channeling technique. At surface temperatures slightly below 600°C, full recrystallization of the implanted layers has been obtained. This result corresponds to the expected temperature for a solid phase epitaxial regrowth of an amorphous layer of 100 nm, produced by the implantation of 5×10^{14} cm^{-2} P^+-ions at 50 keV. Furnace annealing at 350°C is necessary for recrystallization, which is confirmed also by RBS-measurements.

The electrical properties of the implanted layers were investigated by HALL-measurements.

Fig.2 shows the sheet carrier concentration of implanted and annealed layers at about 100 K. Total electrical activation is achieved at surface temperatures of 600°C for a flash lamp annealing with preheating. This result is in good aggreement with the RBS results, where the virgin state is approached at 575°C. Furthermore, HALL and RBS investigations show, that flash lamp annealing without preheating requires higher temperatures around 700°C to obtain full electrical activation and to remove the residual damage after recrystallization. The full activation results in a sheet resistivity of 50 Ω, which is comparable to standard Li-diffused layers (10-20 Ω). For the furnace annealing we observe a maximum electrical activation at 350°C and a deactivation at higher temperatures, as shown in Fig.2.

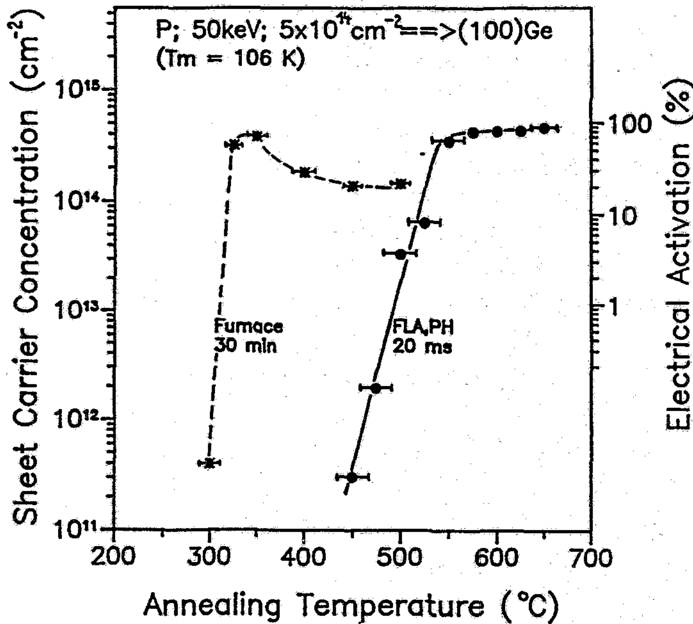

Fig. 2:
Electrical activation and sheet carrier concentration of P^+- implanted and annealed HP-Ge for furnace and flash lamp with preheating

As an example of diode properties a diode current characteristics is given in Fig.3. It has been demonstrated for the first time that completely ion implanted and rapidly thermally annealed diodes can be produced with low reverse currents in the region of pA. Investigation of the capacitance characteristics shows no change of bulk doping even at higher bulk temperatures (>300°C). Full depletion of 700 µm thick diode is measured at reverse voltages of about 3V. According to Fig.3 the diode can be overdepleted with bias voltages up to 20V.

Future investigations will focus on ion implanted detectors with diameters of 10-20 mm and a thickness up to 20 mm in collaboration with INTERTECHIQUE (F).

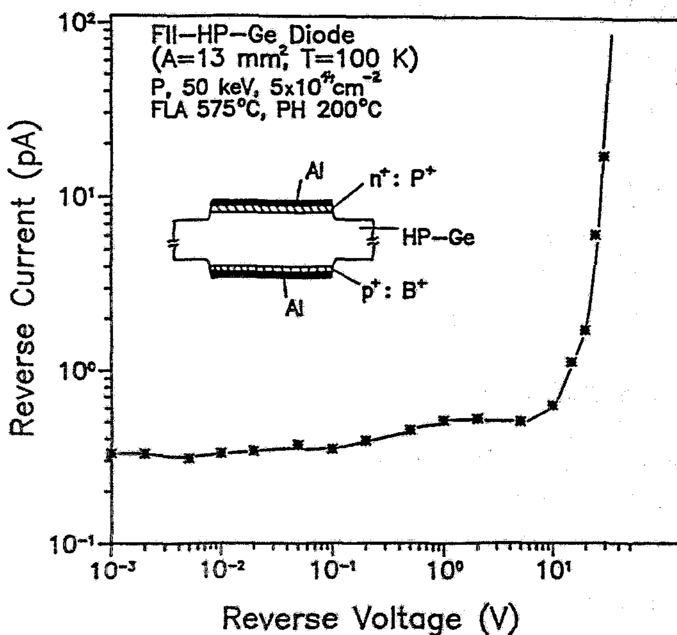

Fig.: 3
Reverse current characteristics of a ion implanted, flash lamp annealed HP-Ge diode (A=14 mm^2) at 100 K

This work has been supported by the BMFT under Contract No. FKZ 06/DR103-TP3

Development of a Fluidic ISFET Microsystem for Chemical Analysis

M. T. Pham and S. Howitz

The Fluidic ISFET Microsystem (FIM) is a microinstrumentation for dynamic multiion detection of electrolyte solutions. The geometrical and electronical design of FIM will be able to integrate chemical microsensors of one or different types. Possible chemical microsensors in FIM are ion-sensitive field effect transistors (ISFETs), micro clark electrodes or micro photometer elements using fiber optics. The direct objective of the project is to initiate a practical use of ISFETs in fields like water analysis or biomedical applications. The development of the FIM components requires in different fields:

- the multicomponent detection by integration of microsensors with different ion sensitivity,
- the prolongation of lifetime by using redundant sensors and actuators,
- the realization of an in-situ calibration for compensating the base-line drift,
- the employment of dynamic measurements for eleminating a conventional reference electrode,
- the sensor encapsulation and microsystem packaging by full wafer level processing.

FIM is of planar design and modularly arranged including four major components: the microfluidic cell, microactuators, microsensors, and the data collection electronics. (see Fig.1)

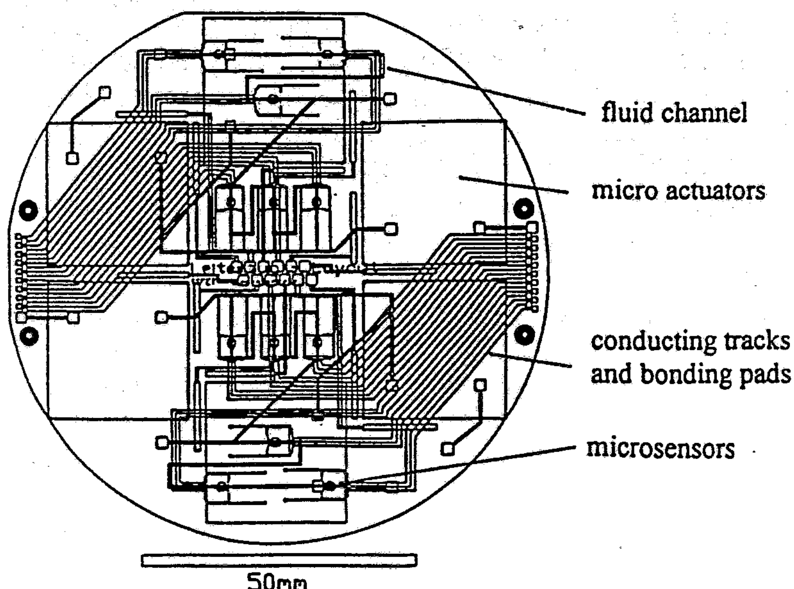

Fig.1: Layout and configuration of FIM. All components are integrated on a 4-" silicon wafer. Micro trenches (200 x 500 μm^2) were anisotropically etched in KOH solutions, finally cove-red with a Pyrex 7740 glass by anodic bonding to form the fluidic microcell.

The FIM concept of in-situ calibration makes use of the well-known procedure of flow injection analysis, modified for multicomponent detection with chemical microsensors. A difference signal is generated by two identical sensors placed in two different fluid channels, where one is flushed by the reference solution. The schematic cross sectional view of a micro fluid channel with two integrated ISFETs and one microactuator is shown in Fig.2. Microsensors, microelectronics and Al-contacting paths are located on the silicon wafer, microactuators and the fluid inlets and outlets are placed on the opposite glass side. A spacer-chip technique has been developed for the integration of microsensors and microactors of different geometry into the FIM assembly.

The system functionality was testet with a FIM prototype comprising a fluid microcell with 6 pH ISFETs and 6 pNO_3 ISFETs. The internal fluid handling was realized by three piezoelec-

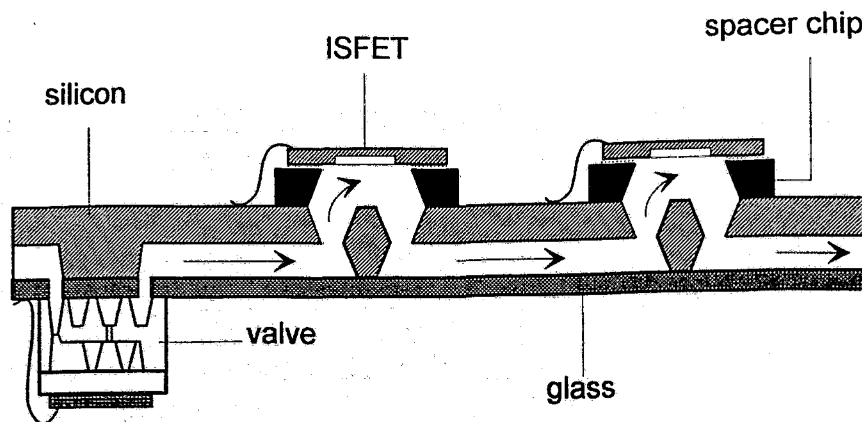

Fig.2: Schematic cross sectional view through an FIM flow cell.

tric microcroactuators during the pH measurements. For the detection of nitrate, a preliminary external fluid handling system was used. The signal processing electronics were first realized by a macro version of an ASIC module. An example of the nitrate measurements with the FIM prototype is shown in Fig. 3.
Results obtained from measurements with pH ISFETs integrated in FIM over a period of three months demonstrate that the system meets the requirements for routine analysis regarding accuracy, reproducibility and capability of the fluid handling procedure. Most problematic for the operation in the sub-micronliter regime appear the membrane microvalves causing leakage and thus limiting the detection resolution. For fluid handling in the nanoliter range, we succeeded in developing a fluid manipulator consisting of a piezoelectric injector and a fluid diode which is able to supply liquids without any leakage. The activation of redundant sensors is possible by the anodic dissolution of a thin metal layer covering the ion sensitive membrane. Multicomponent detection will be is feasible by using microsensors for other species including also optical chemo- and biosensors in future.

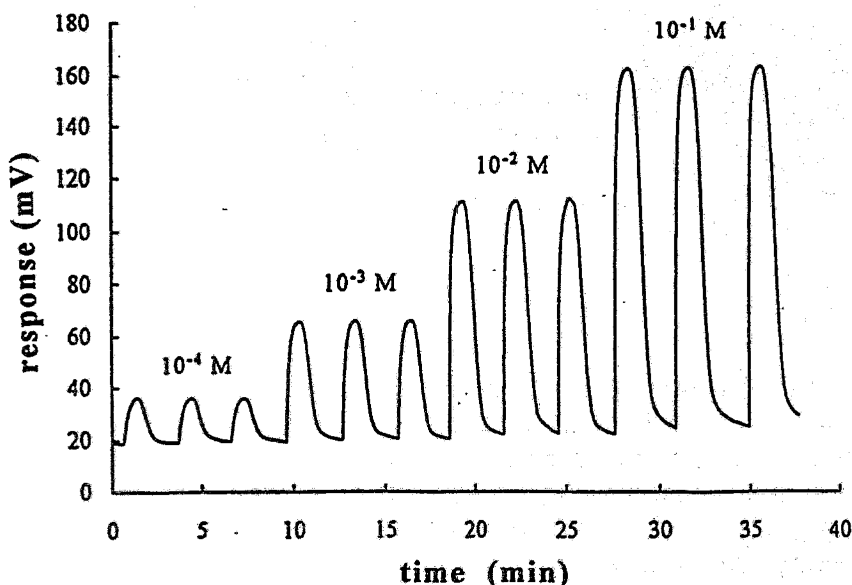

Fig. 3: Dynamic differential measurement of nitrate with pNO_3 ISFETs integrated in FIM: flow rate 0.5 ml/min, sample volume 500 μl, carrier 10^{-5} M KNO_3 in 0.1 M $(NH_4)_2SO_4$

FIM is a joint project financially supported by the SMWA.

Depth Selective Mössbauer Spectroscopy on Al–implanted Iron

H. Reuther, O. Nikolov [*], S. Kruijer [**], R.A. Brand [**] and W. Keune [**]

[*] Institute of Nuclear Research, Sofia, Bulgaria
[**] Laboratorium für Angewandte Physik, Universität Duisburg, Germany

Iron rich Fe–Al alloys are very interesting because of their magnetic properties. They can be produced by Al implantation into α–Fe surfaces. Both implantation parameters (energy, dose, current density) and implantation conditions (temperature, heat flow) have an important influence on the structure of the layer produced. To obtain informations on the various alloy phases and on the depth distribution of the different phases within it ^{57}Fe conversion electron Mössbauer spectroscopy (CEMS) and depth selective CEMS (DCEMS) was applied. The implantation depth profiles were measured by Auger electron spectroscopy (AES) using the new MICROLAB 310 F.
All samples were implanted with the same nominal dose of $5x10^{17}$ cm^{-2} Al^+ ions at an energy of 50 keV and a current density of 3.7 $\mu A/cm^2$; however, the shape of the specimens and the mounting conditions were different from sample to sample. The thermal contact during the implantation varied from very bad for sample 1 (clamped to the target holder with springs) to very good for sample 5 (fixed with silver glue to an Al disk, held on the target holder with vacuum grease). Both natural and enriched to 95% in ^{57}Fe iron foils were used to get reasonable counting times for DCEMS.
The CEM spectra (Fig.1) may be described by three spectral components, namely a broad central single line (phase 1), a magnetically– split component with a hyperfine field distribution $P(B_{hf})$ (phase 2), and the α–Fe sextet of the matrix.
The first component can be assigned to a non–magnetic alloy with an Al concentration above c_{cr} = 33 at.–% Al and the second to a disordered alloy with an Al concentration below c_{cr}. It is obvious from Fig. 1 that the relative intensity of the central non–magnetic line increases if the thermal contact of the sample to the target holder during implantation becomes worse.
Sample 1 has been studied in detail by DCEMS in the L–conversion electron range. A clear energy dependence of the DCEM spectra is observed (Fig. 2). As in the case of the CEM spectra in Fig. 1, the DCEM spectra were analysed in terms of three spectral components. The relative intensity of the central single line corresponding to a non–magnetic alloy with high Al concentration is generally reduced with decreasing electron energy providing evidence that this phase is located near the surface.
The concentration profiles for all samples measured by AES were nearly identical. In Fig. 3 the depth profile of sample 5 is shown as an example. It indicates two interesting aspects: (i) the maximum Al concentration is very high (more than 50 at.%) and the Al profile extends to a very large depth (more than 200 nm); (ii) a considerable amount of oxygen is observed (about 25 at% at the surface) extending relatively deep into the sample.
Standard TRIM calculations yielded an Al concentration profile with a maximum at a depth of 33 nm with a longitudinal straggling of only 20 nm. It is supposed that the large Al penetration depth observed is the effect of radiation–enhanced diffusion taking place even at the slightly raised target temperature during implantation. The high oxygen content is attributed to the Al implantation too, because both untreated and Si implanted Fe samples did not show an oxygen profile. It is likely that the relatively great chemical affinity of aluminium for oxygen leads, on the one hand, to the high Al content near the surface, and on the other hand, to the inclusion of oxygen. This process may have been stimulated by the radiation damages due to the ion implantation.

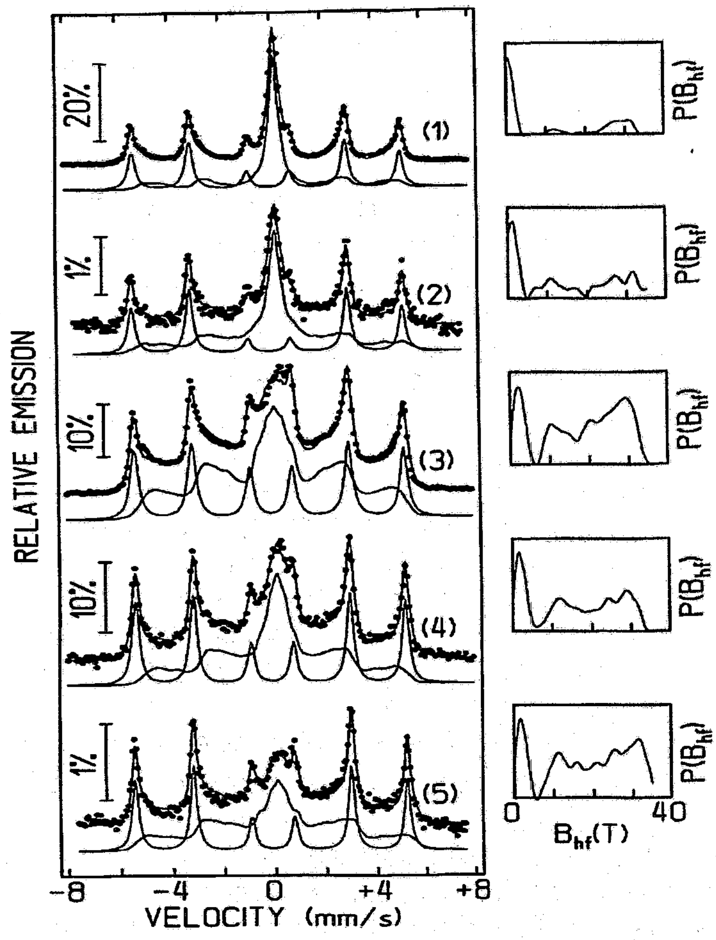

Fig. 1: CEM spectra of the Al implanted samples No. 1–5 at 300 K and least-squares fit hyperfine field distributions

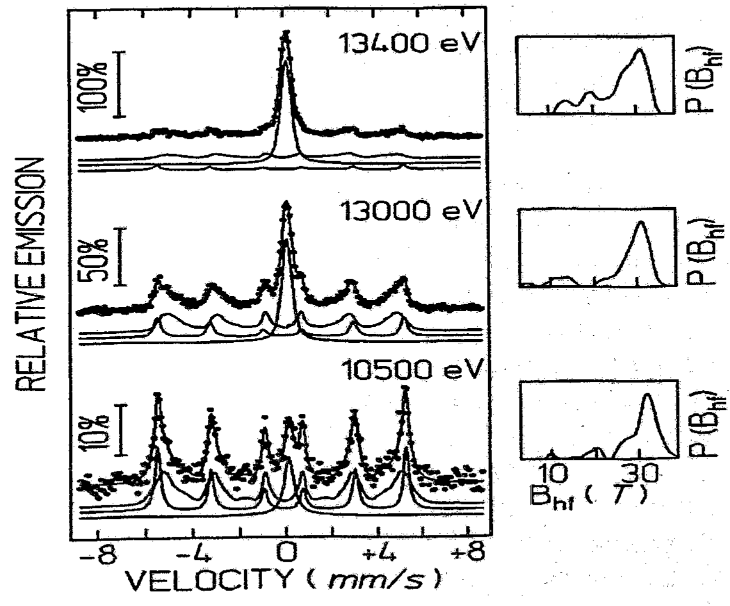

Fig. 2: DCEM spectra of sample 1 at 300 K and least-squares fit hyperfine field distributions at various selected electron energy settings V

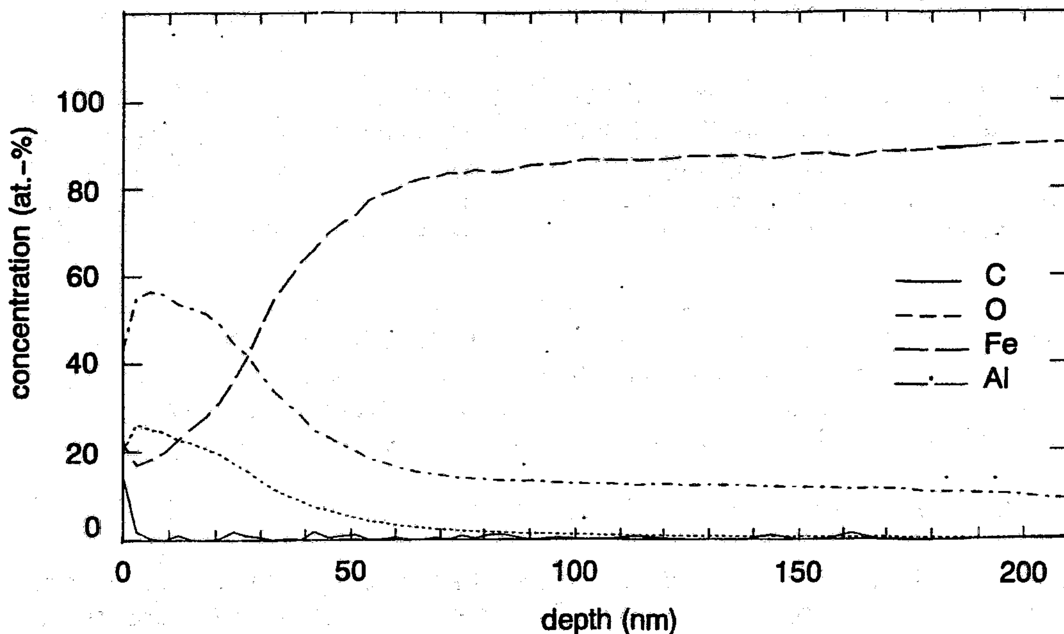

Fig. 3: Concentration depth profiles for Al, Fe, and O of sample 5 measured by AES

The measured absolute CEM spectrum areas of the three spectral components were compared with areas computed on base of theoretical calculations using weight functions of the electron–energy dependence for the detected conversion electrons [1]. A surprisingly good agreement was found under the following main assumptions: (i) all of the oxygen has reacted exclusively with Al to Al_2O_3, and not with Fe (since no iron oxide was observed in the CEM spectra). (ii) The residual Al belongs to Fe–Al phases. (iii) Within the first 91 nm below the surface only phase 1 and between 91 and 185 nm only phase 2 exist. For depths larger than 185 nm only the α–Fe phase is present.
The conclusion is that, contrary to overlapping structures normally arisen from ion implantation, really a layer structure was produced. Further work has to be done to investigate the process of oxygen inclusion into the sample.

This work was supported by the Deutsche Forschungsgemeinschaft, Bonn.

Reference

[1] H. Reuther, O. Nikolov, S. Kruijer, R.A. Brand, W. Keune, D. Liljequist, S. Weber, and S. Scherrer, Hyperfine Interactions, in preparation

Plasma Source Ion Implantation

R. Günzel, E. Wieser, E. Richter, and J. Steffen

Ion implantation, e. g. the implantation of N^+ in iron or steel, is a common method used to improve the mechanical properties of metal surfaces. The formation of AlN precipitates in the near surface region of aluminium by ion implantation has been shown to improve the mechanical properties in this respect. An increase in hardness and reduced wear has been obtained for example by irradiation of aluminium with a beam of 90 or 80 keV N^+/N_2^+ ions [1,2].

In addition to the conventional ion implantation technique the plasma source ion implantation (PSII) method is of growing importance due to several advantagous effects such as the homogeneity of implants for targets with complex geometry. Therefore it seems appealing to apply this promising technique to improve the surface properties of aluminium. The first successful experiment on PSII of nitrogen into aluminium and aluminium alloys has been reported [3].

This preliminary study reports on the first PSII performed in Germany.

PSII of nitrogen in aluminium was carried out in a 15 l chamber using a plasma generated by a filament assisted DC discharge (arc current 6 A) . The pressure within the chamber was 2 Pa. The sample was biased by negative voltage pulses of 35 kV maximum with a pulse duration of 20 µs (time for the voltage decrease down to half maximum) and a repetition rate of 100 Hz. The average current during a voltage pulse was about 1 A corresponding to a current density of 60 mA/cm². The average current during experiment was about 5 mA. The samples were heated during the implantation to 200 +/- 50°C by the absorbed power . In order to prepare samples with different ion doses the implantation time was varied between 500 s and 3000 s.

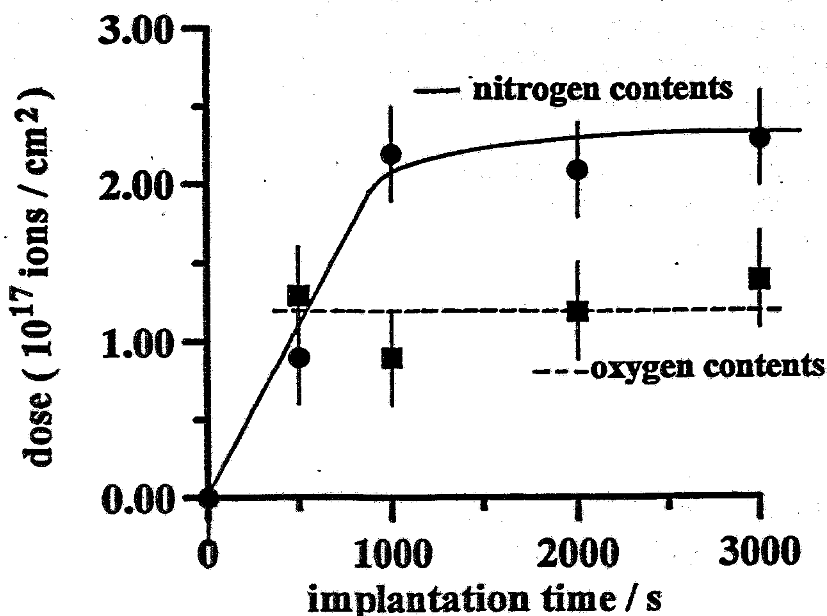

Fig. 1 Nitrogen and oxygen areal densities obtained by PSII of nitrogen for different implantation times

Aluminium discs of 30mm diameter and 2 mm thickness from semihard 99.5Al were first mechanically polished and then electrochemically polished on both sides.
The nitrogen and oxygen areal densities obtained by PSII of nitrogen for different implantation times are shown in Fig. 1. An increase of the nitrogen dose with increasing time is only observed from 500s to 1000s. After approximately 1000s a saturation in the dose of the implanted species is achieved. Additional a relatively high oxygen dose, independent of the implantation time is measured.
In Fig. 2 AES depth profiles are shown after PSII for 3000 s, an implantation time at which saturation of the nitrogen dose has been achieved.

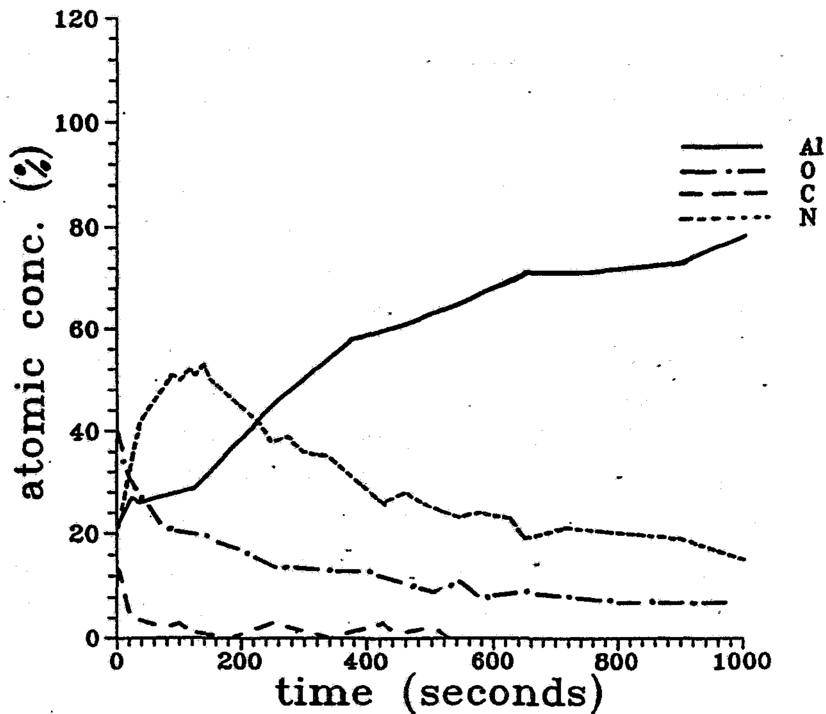

Fig. 2 AES depth profiles of C, O, N and AL measured after PSII of nitrogen for 3000 s

The concentration of nitrogen and oxygen in a thin surface layer is approximately 50 at % and 20 at % respectively. Thus it is most likely, that a uniform layer of nitrides and oxides has been formed, consuming all available metallic aluminium.
The nitrogen and oxygen concentrations of Fig. 2 are gradually decreasing with depth and after 2000 s sputter time (not shown here) no oxygen or nitrogen was measured.
The sputter conditions of the spectrometer refer to a corresponding sputter yield of Ta_2O_5 of 0.25 nm/s. Measurement of the depth of the sputter cone leads to a sputter yield of the aluminium sample of about 0.8 nm/s.
The maximal concentration of nitrogen was measured after 120 s, thus corresponding to a depth of 96 nm, in agreement with the mean projected range of 35 keV nitrogen ions in aluminium of about 90 nm [4].
Further investigations are necessary to clarify the deep penetration of the nitrogen ions into the bulk material, as well as the origin of the obtained oxygen concentration profile (Fig. 2).
On the one hand the obtained oxygen dose is nearly independent of the implantation time (Fig. 1), and on the other hand the concentration profile is decreasing with depth, similar to the concentration profile of nitrogen.

References:

[1] I. Kanno, K. Nomoto, S. Nishijima, T. Nishiura, T. Okada, K. Katagiri, H. Mori, and K. Iwamoto, Nucl. Instr. and Meth.B 59/60 (1991) 920

[2] M. Braun, Nucl. Instr. and Meth. B 59/60 (1991) 914

[3] J.R. Conrad, PSII Newsletter 4 (1993) 6, Plasma Source Ion Implantation Laboratory, University of Wisconsin.

[4] J. F. Ziegler, J. P. Biersack and U. Littmark, The Stopping and Range of Ions in Solids, Pergamon Press N. Y. (1985)

Simultaneous Light Element Analysis by HIERD for Plasma-Wall Interaction Studies in Fusion Research

U. Kreissig, R. Grötzschel, R. Behrisch*, S. Grigull

*) *Max-Planck-Institut für Plasmaphysik, EURATOM Association, Garching*

In thermonuclear fusion research using Tokamak plants it is tried to confine a D-T plasma at very high temperatures by strong magnetic fields [1]. However the magnetic confinement is limited and therefore the plasma-facing areas of the inner vessel wall are bombarded by plasma ions and energetic neutrals, causing implantation and erosion. The eroded material enters the plasma, but is finally redeposited on the vessel wall together with other plasma impurities such as oxygen, and plasma ions. The plasma-facing areas are generally covered with tiles made from low-Z elements, which can be easier tolerated in the plasma than high-Z elements.

For a quantitative investigation of implantation, erosion and redeposition processes a fast, reliable and quantitative analysis of all the low-Z elements is necessary. The most straightforward method to measure simultaneously the amount and the depth distribution of different light atoms trapped in the surface layers of a solid is the Heavy Ion Elastic Recoil Detection technique (HIERD) [2-4]. The physical base of this method is the elastic scattering of energetic ions, but in difference to RBS the recoil atoms ejected from the sample are detected. Using two different detection methods for the recoils, we were able to analyze simultaneously all light elements in a sample from the hydrogen isotopes up to oxygen.

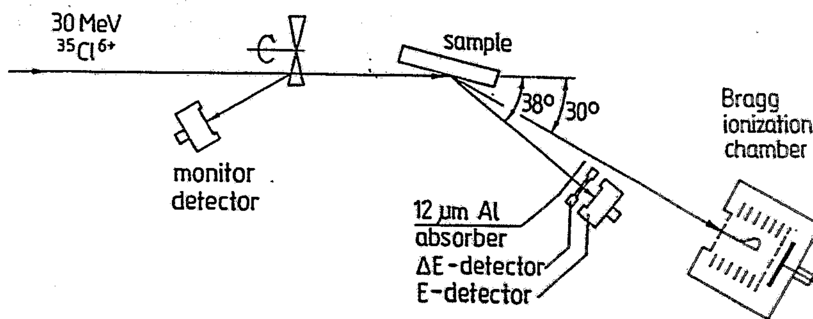

Fig. 1 Experimental setup for HIERD using particle identifying detection methods

The measurements have been performed with 30 MeV ^{35}Cl ions at our 5 MV tandem accelerator. Fig. 1 shows the experimental setup using the typical ERD geometry with glancing angle incidence of the ion beam. Two detectors were used for identification and spectroscopy of the recoil atoms. Hydrogen and helium isotopes were detected by a ΔE-E telescope under Θ=38°. It consists of a 14µm thick Si transmission detector followed by a SSB detector with a sensitive depth of 500µm. A 12µm thick Al foil protects the telescope against backscattered Cl ions and recoils heavier than He. For Z= 3...11 elements a Bragg Ionisation Chamber (BIC) similar to that described earlier by Hentschel [5] was used, positioned under Θ

=30° with respect to the incident ion beam. Beam currents of some nA were typically applied. The backscattered Cl ions from a rotating beam shutter served for normalization of the spectra. The ΔE- and E-signals from the telescope and the E-signals from the BIC were processed by standard NIM electronics. For the Bragg-peak signal a special amplifier with shaping time constants between 47 and 220 ns was used. For each detector system a 2D-spectrum with a resolution of 256x256 channels, representing ΔE vs. E for the telescope and Z vs. E for the BIC was recorded.

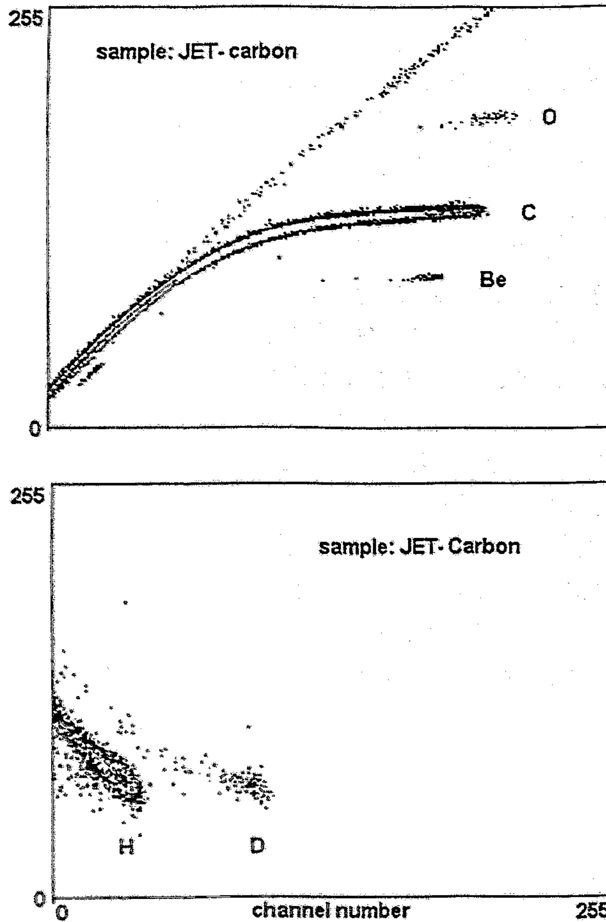

Fig. 2 2-dim. spectra from simultaneous BIC- (above) and ΔE-E telescope measurements of a carbon sample from the JET fusion plant. In both cases, the vertical axis serves for identification of the recoiling ions.

Fig. 2 shows the 2D-spectra of different light elements from BIC- and hydrogen isotopes from ΔE-E telescope measurements of a carbon sample extracted from a divertor plate of the European fusion plant JET in Culham after deuterium plasma operation including few discharges with tritium admixture. As for the BIC data, three well separated branches of O, Be and the matrix component C can be recognized. The Be originates fom the plasma erosion of Be components also present in the Tokamak vessel and its redeposition onto the carbon surface. Oxygen is a main plasma impurity. It will be gettered preferably by the Be in the surface region. In the ΔE-E spectrum recorded simultaneously, no evidence of a tritium content can be found while the discrimination of T recoils from ^{1}H and D isotopes could be demonstrated with other samples [7]. This indicates a successful "cleaning" by subsequent deuterium operation. However, it should be mentioned that the detection sensitivity for tritium is less by a factor of ~20 compared to ^{1}H.

In order to derive the impurity concentration profiles, the respective recoil branches as shown in Fig. 2 are projected separately onto the energy axis, thus yielding single element spectra. We calculate the elemental distributions directly from the spectral yield Y(E) by means of a 2-axis transformation, involving elastic scattering kinematics, cross-sections and energy dependent stopping power data [8] as input information. The contribution of the trapped atoms to the ion stopping is accounted for via an iteration procedure which is basically self-

consistent as the total stopping power within the target is modified according to the calculated depth distribution of each element and vice versa. In the case of the JET-material, this requires a simultaneous analysis of both telescope and BIC data. Fig. 3 shows a set of concentration

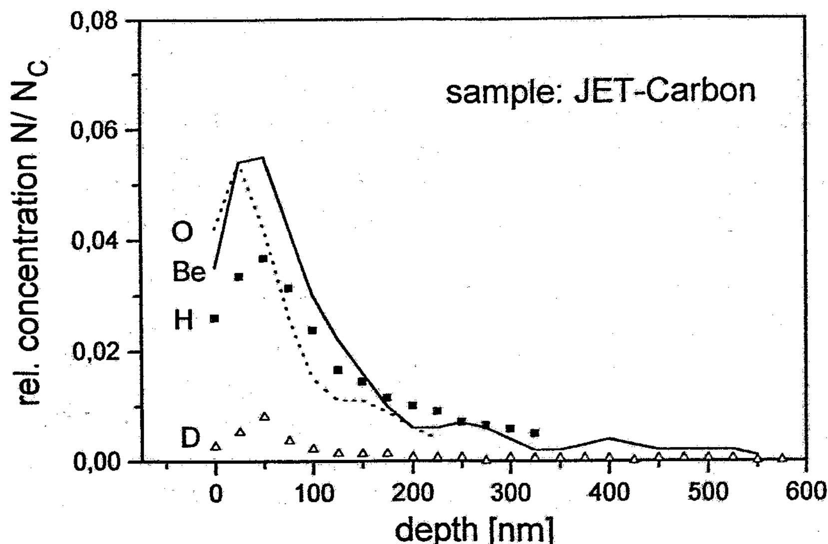

Fig. 3 **Depth distribution of low-Z impurities in a JET-carbon sample. The concentrations are normalized to the matrix material with 100nm corresponding to 1.1×10^{18} at/ cm^2.**

profiles of the detected elements Be, O, ^{1}H and D derived from the above spectra. Because of the linear dependence of energy loss on the target density, nanometer depth scaling necessitates either assumptions on or extra measurements of the matrix density which may considerably deviate from tabulated values in the analyzed region. Independent of the impurity species, the respective maximum concentration is believed to shift to the surface when the spectra are deconvoluted prior to the profiling procedure.

References:

[1] F. Engelmann in : Physics of Plasma Wall Interaction in Controlled Fusion, eds. R. Behrisch and D. Post, Pergamon, 1987, p. 15

[2] F.H.P.M. Habraken, Proc. 2. Europ. Conf. on Accelerators in Appl. Res. and Technology, North-Holland, 1992, p.181

[3] E. Arai, H. Funaki, M. Katayama, and K. Shimizu, ibid. p.202

[4] M. Alurralde, E. Garcia, D. Abriola, A. Filevich, G. Garcia Bermudez, M. Aucouturier and J. Siejka, Conf. Proc. High Energy and Heavy Ion Beams in Materias Analysis, MRS 1990, p. 119

[5] E. Hentschel, R. Kotte, H.G. Ortlepp, F. Stary and D. Wohlfahrt, Nucl. Instr. and Meth. B 43 (1989) 82

[6] The JET team, Nul. Fus. 32 (1992) 187

[7] U. Kreissig, R. Grötzschel, R. Behrisch, to be published in NIM B

[8] J.F. Ziegler, J.P. Biersack, U. Littmark, The Stopping and Range of Ions in Solids, Vol. 1, Pergamon Press, N.Y., 1985

Paint Layer Studies using PIXE on Air

C. Neelmeijer, W. Wagner, H.-P. Schramm

Originally, the PIXE (Proton Induced X-ray Emission) technique was developed to study thin films (aerosol, serum - d<0.1μm) on light substrates (organic foils, carbon backings) or thick homogeneous targets like minerals. The present work reports on first results gained on extended paint layer systems by means of the external proton beam. PIXE on air allows the substantial analysis on details of art objects in a non-destructive manner [1]. Analyzing paintings the advantages and limitations of this technique we reported already earlier [2].

Oil paintings represent one of the most complicated and unique art objects for the analyst. Preparing cross sections one observes pigment multilayer structures on a chalk grounded carrier as wood, textile or paper. The individual paint layer consists of an inorganic pigment or a pigment mixture (metal oxides, metallic salts) in connection with about 30% of organic binders (resin acids); the uppermost paint layer is typically covered by an organic varnish film [3]. Very different paint layer thicknesses have been obtained varying in the order of microns up to some 10 μm....100 μm. The lateral dimensions of analytical interest amount to tenth of one millimeter up to some millimeter.

The answer of the question whether certain pigment elements observed are arranged in multilayers or mixed in one paint layer should be possible by X-ray excitation varying the information depth, i.e. by PIXE measurements at different incident proton energies $E_{p,o}$. Calculations show that the investigated depth region at a given $E_{p,o}$ is mainly determined by the proton energy loss in the paint material defining the x-ray production cross section $\sigma_x(E_p(t))$ in dependence on E_p at depth t . To check the evidence of this idea a set of test paint layers containing combinations of typical pigments was prepared (Fig.1) and subsequently analysed using beams of 3 MeV and 2 MeV primary protons [4]. After passing through the 8 μm thick KAPTON exit foil and 1.5 cm of air incident energies of $E_{p,o}$ = 2.5 MeV and 1.4 MeV were available, respectively.

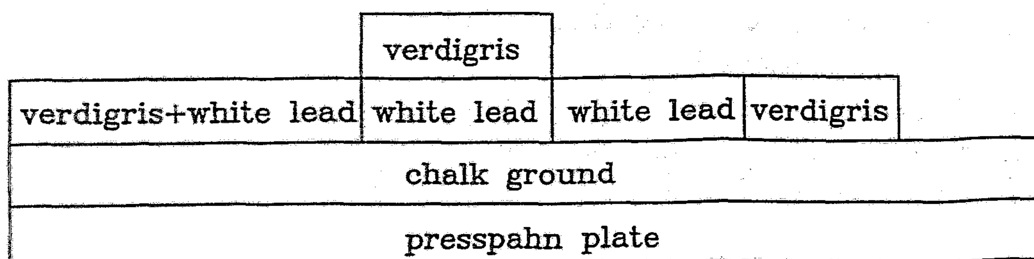

Fig.1: Schematical sketch of several test paint layer structures including the pigments verdigris $\{Cu(CH_3COO)_2 \cdot H_2O\}$ and white lead $\{2PbCO_3 \cdot Pb(OH)_2\}$ on $CaCO_3$

The X-rays were measured by a Si(Li) detector at 135° backward angle. Fig.2 compares the PIXE spectra taken from the verdigris on white lead double pigment layer arrangement (Fig.1) at 3 MeV and 2 MeV primary proton energy.

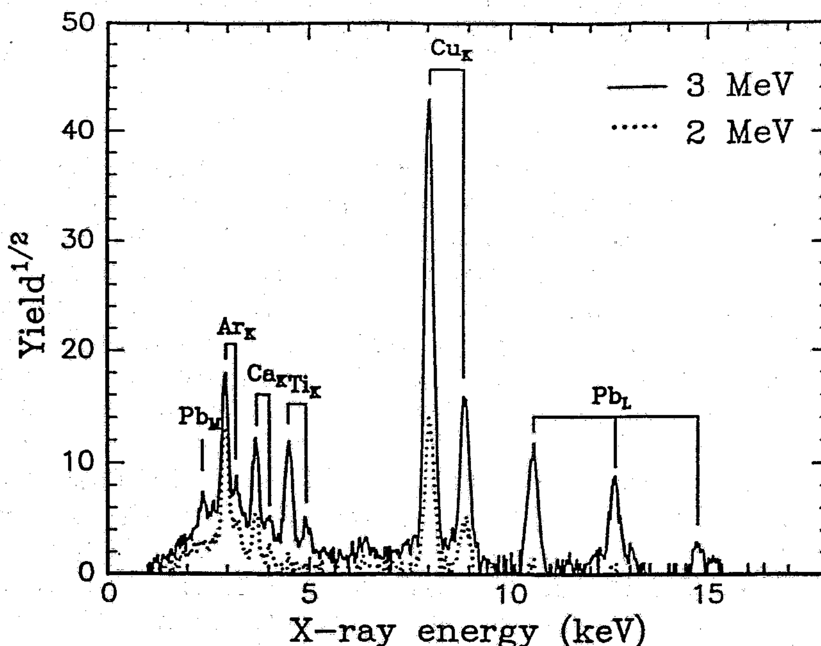

Fig.2: X-ray spectra from the double pigment layer system {verdigris on white lead} deposited on chalk ground - Measurements at 3 MeV and 2 MeV primary proton energy

The thick target option of the GUPIX evaluation program [5] was used for quantitative analysis of the measured PIXE spectra. Tab.1 presents the relative elemental concentrations derived from Fig.2 for the layer structure verdigris/white lead/chalk.

Tab1: Relative concentrations (at%) of elements visible in the PIXE spectrum (Fig.2); for calculation of stopping and absorption the full pigment composition as well as a 30% portion of binding agents {$C_{30}H_{50}O_2$} were fed in GUPIX

primary proton energy	Ca	Ti	Cu	Pb
3 MeV	2%	2%	50%	46%
2 MeV	3%	-	97%	-

At the higher proton energy both the Cu-K and Pb-L radiations are dominant. Note the low Pb-M intensity, in relation to the Pb-L radiation yield, as a first fingerprint for a strong attenuation of this low energy x-radiation as a consequence of buried Pb atoms. Additionally, Ar-

(from air), Ca- and Ti-K radiation appears. At the lower proton energy the Pb signals (Pb-L, Pb-M) vanish completely. This is due to the proton energy loss (σ_x breaks down for inner layers) and x-ray absorption within the verdigris overlayer. The Ti-K signal also disappears at 2 MeV proton energy; we interprete titanium (possibly titanium white) as an impurity or admixture within the lead white pigment. From the constant fraction of calcium, independent on the proton energy, we attribute the Ca-K X-radiation to origin from an impurity within the paint material and not from the chalk ground.

Generally, including an absolute efficiency calibration of the detector arrangement and counting the total number of impinging protons, at least at the maximum primary proton energy, GUPIX allows to calculate the absolute areal density $N(Z_i)$ (at/cm^2) of matrix atoms Z_i . From this, paint layer depths can be deduced by the GUPIX program when taking into account representative density values (g/cm^3) of the paint substances [3]. This idea will be pursued in the near future. To check the layer thicknesses determined by PIXE in this manner comparisons with depth evaluations by optical microscopy on cross sections from the test paint structures (Fig.1) are in preparation.

The example (Fig.1) demonstrates that a paint layer system can be non-destructively studied by PIXE on air. White lead and verdigris are typical pigments used since the Antiquity . Other test layer structures including elements of the later pigment chemistry, e.g. zinc white/chromium oxide/chalk known since the 19th century, were also successfully analysed. With this experiences, the technique of proton beam energy variation will be applied in connection with PIXE analysis on original paintings of Lucas Cranach.

This work is supported by the BMFT under contract 215-4003-NE9ROS

[1] M. Menu, Nucl. Instr. Meth. B75 (1993) 469
[2] H.-P. Schramm, C. Neelmeijer, H. Matthes, W. Pfestorf, in: Wiener Berichte über Naturwissenschaften in der Kunst, Wien:VWGÖ, vol. 4/5 (1987,88) p. 26
[3] H.-P. Schramm, B. Hering: Historische Malmaterialien und ihre Identifizierung, ADVA Graz, 1989
[4] The measurements were taken at AGLAE - Laboratoire des Recherches de Louvre, Paris, Frankreich
[5] J.A. Maxwell, J.A. Campbell, W.J. Teesdale; Nucl. Instr. and Meth. B43 (1989) 218

Texture Investigation on Geological Three Phase Samples

K. Ullemeyer, M. Betzl, J. Heinitz, and K. Walther

Geological deformation processes have been acting in the far past, in large depths, or under other extreme conditions. Therefore they cannot be studied directly. Since texture contains information about the deformation history, its investigation represents an important tool for the understanding of the processes in the earth's crust. The present paper reports on texture investigations of four polyphase geological samples containing quartz, plagioclase, and biotite.

For the investigation of the preferred orientation of crystallites in geological bulk samples is the prefearable method. Its large cross section of the neutron beams allow the investigation of coarse grain samples and samples with inhomogenities.

Geological samples are mostly of low crystallographic symmetry which results in many overlapped BRAGG peaks in the diffraction pattern. The neutron time-of-flight (TOF) method has significantly better resolution than the standard two-axis diffractometry. Furthermore, with TOF-diffractometry all possible BRAGG reflections are measured simultaneously. Therefore TOF has been choosen for the present investigations.

Pole figures are obtained at the time-of-flight diffractometer NSHR [1] at the pulsed reactor IBR-2 of the Joint Institute of Nuclear Research in Dubna, Russia. The samples were cut to a cylindrical shape with 25 mm diameter and 22 mm length and mounted in a texture cradle. In order to measure complete pole figures the sample rotation was repeated with different orientations of the axis of rotation with respect to the scattering vector. The typical exposure time for the data acquisition was 20 minutes. Using a resolution of 7.2 x 7.2 degrees, 700 diffraction patterns of each sample were obtained. From these, 18 pole figures are extracted by calculating the peak intensities. Despite of the high resolution of the NSHR diffractometer, there are many overlapped peaks. The extracted experimental pole figures are superpositions of pole figures of two or of all three phases in most cases, or they are superpositions of several pole figures of different peaks of the same phase.

Figure 1 illustrates the geological coordinate system which is commonly employed. The XY plane is the foliation plane, where X is the lineation direction. Pole figures are generally given in section XZ. Describing a deformation, these axes represent the main axes of the deformation tensor.

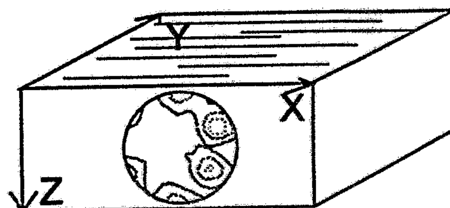

Fig. 1 The geological sample coordinate system. The XY plane is the foliation plane, the X direction is the lineation direction.

In Fig. 2 are shown some pole figures of one of the samples. These pole figures show deviation to the above mentioned ideal deformation processes. The biotite (001) pole figure has sharp (nearly axialsymmetric) maxima in Z direction. This refers to only one dominant foliation. The axial symmetry points to oblate and/or very high strain. In the quartz (110) pole figure the significant maxima are located near X and show circular symmetry. There is no trend to elongation on small circles, which would indicate oblate strain. Contrary to the biotite pole figure, this refers to a plain deformation Furthermore this texture is characterized by the fact, that in the (110) pole figure the great circle connecting the maxima is declined from the XZ plane. Correspondingly, the maximum is shifted from the centre also in the (001) pole figure.

These observations on the biotite and quartz texture can interprated in the following way: the biotite (001) pole figure reflects the total bulk strain. In contrast, the quartz texture shows only the last strain increment. Only in an oblique deformation regime the axes of the incremental strain tensor deviate from the axes of the bulk strain tensor, i. e. in such cases the quartz texture is an indicator for an oblique deformation regime. The interpretation of the plagioclase texture is at the state of beginning. Evidently, the texture exhibits a maximum in the (101) pole figure at Z. This points to a (10) plane as dominant slip plane.

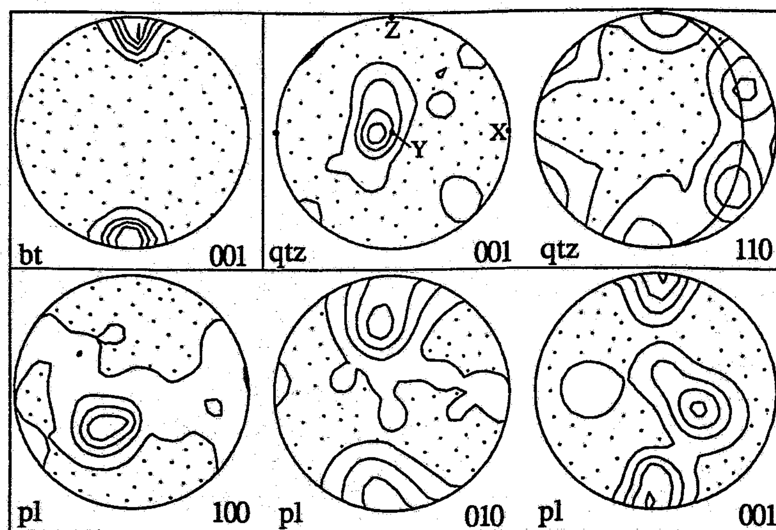

Fig. 2 Recalculated pole figures of a sample containig biotite, quartz, and plagioclase

Summarizing can be stated, that neutron time-of-flight diffraction at high resolution diffractometers is a very good tool for texture investigation of polyphase samples and/or materials with a low crystallographic symmetry.

[1] K. Helming, W. Voitus, and K. Walther, Physica B, 180 & 181 (1992) 1025

Status of the Rossendorf 7.25 GHz ECR Ion Source: Measurement of Electron Energy Distribution and Characteristic X-Ray Spectra

H. Tyrroff, D. Henke, R. Friedlein*, St. Herpich*, H. Hiller* and G. Zschornack*
* Institut für Kern- und Teilchenphysik der TU Dresden

A 7.25 GHz ECR ion source [1] being in operation at Rossendorf since '93 was tuned to obtain highest possible charge states.
For this reason the source was equipped with an analyzing magnet, a Faraday cup and a beam scanner to measure charge distribution spectra and to observe the beam profile and its position. The discharge was confined by grids to maintain a volume pressure below 10^{-6} mbar reducing recombination. Additional electrons are generated from an isolated disk movable into the ECR zone. The dependence of the charge distribution of the extracted beam on the working gas pressure and the mixing ratio with the cooling gas have been examinated for different mirror field strength and rf power levels. Voltage and position of the movable disk were optimized. Table 1 shows the highest charge states obtained so far.

Tab. 1: Highest charge states obtained

Element	He	N	O	Ar	Kr	Xe
qmax	2	6	5	11	15	24
I[eμA]	35	6	5	1.5	<1	<1

In order to understand the source behaviour, the elementary processes of ionization and recombination have been analyzed on the base of internal plasma parameters like electron energy distribution and interaction cross sections [2]. This approach describes the charge distribution spectra of an ECR ion source and can explain the internal ion cooling by mixing with gases as well as the pulse driven ECR discharges which use afterglow [3]. Both, cooling and afterglow enhance higher charge states. In order to obtain the electron energy distribution F(E), Bremsstrahlung escaping axially from the 7.25 GHz ECR discharge was strongly collimated to about $5 * 10^{-6}$ sr, analyzed by means of an HP-Ge detector [4]. The spectra were mathematically deconvoluted using an improved method [5] which performs an exact and numerically stable solution of the integral equation for F(E). An example is shown in Fig. 1. It shows the measured Bremsstrahlung spectrum ($P_{measured}$) and the corrected one (P_{corr}) with respect to detector efficiency and the calculated F(E) for the indicated discharge conditions. It was assumed that the composition of the plasma compounds corresponds to the measured of the extracted beam. The slope of F(E) shows a Boltzmann behaviour of the plasma with two temperature components of approximately 3.5 resp. 45 keV. The shape of F(E) is influenced by the radiation scattered at the collimator as indicated in fig. 1.

The influence of gas pressure, rf power, magnetic confinement and gas mixing on F(E) was examined. In this way, by comparing charge distribution and corresponding F(E), we intend to improve the ECR source operation and its understanding.

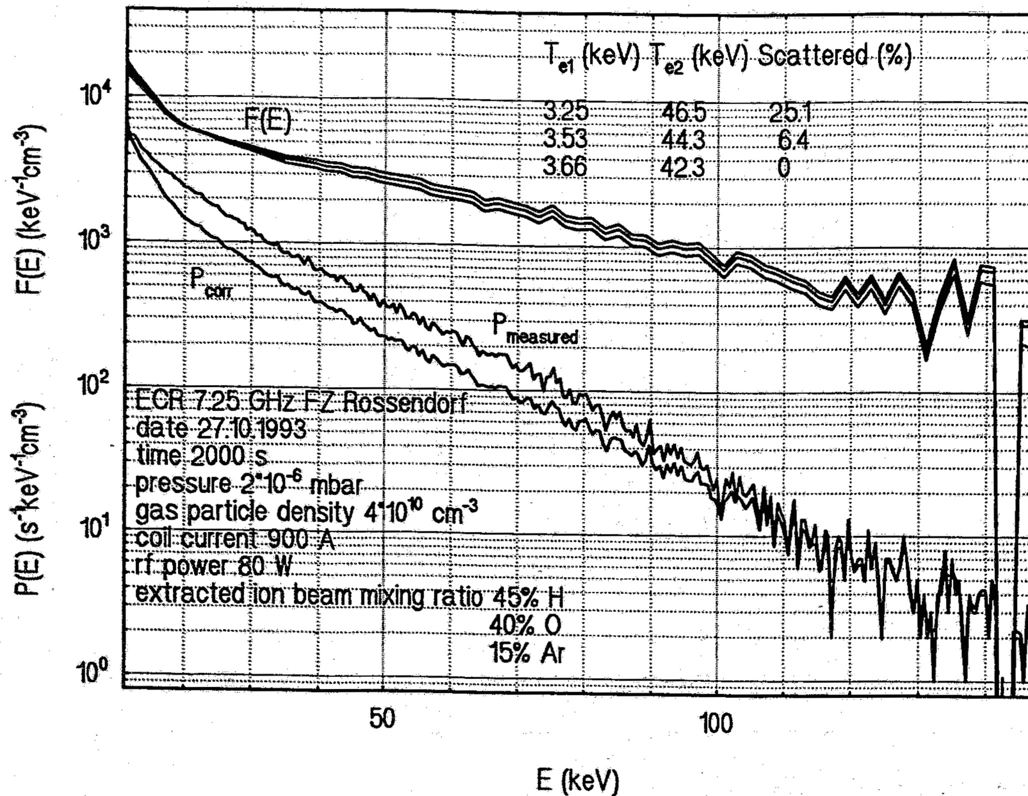

Fig.1 Bremsstrahlung spectrum P(E) and electron energy distribution F(E) for typical ECR discharge conditions

First spectra of characteristic X-rays emitted by rare gas ions inside the 7.25 GHz ECR discharge have been measured by means of HP Ge detector (see Fig. 2).

The intensity of the axially emitted X-rays proved to be strong enough for the use of a crystal diffraction spectrometer in further investigations. The high resolution of this spectrometer permits to compare the ionic charge distribution inside the plasma to the corresponding charge distribution of the extracted ion beam.

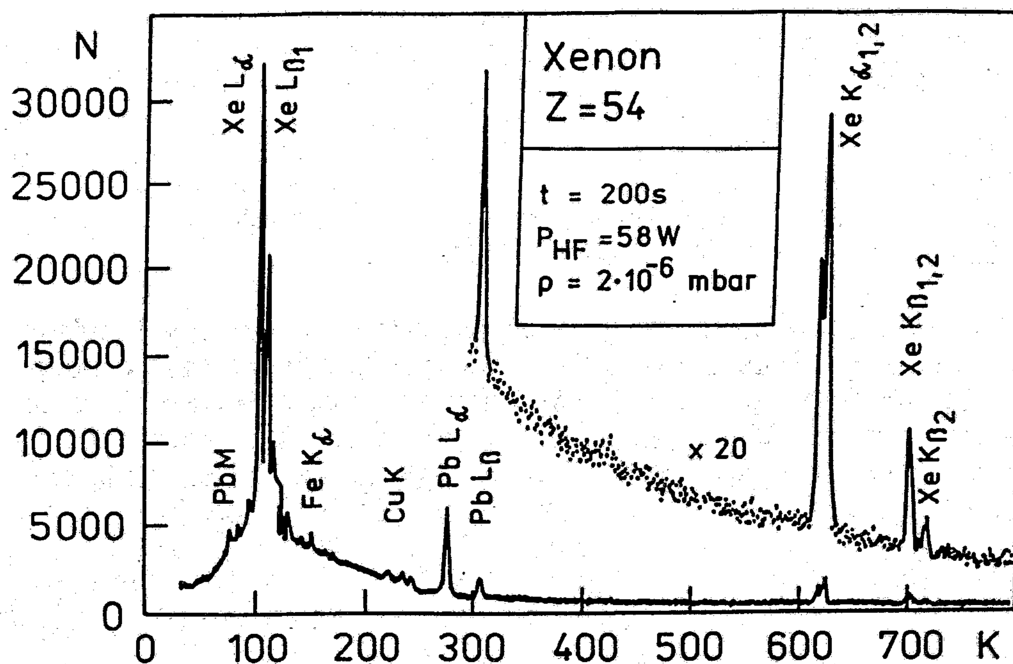

Fig. 2 Characteristic Xenon X-ray spectra emitted by the 7.25 GHz ECR discharge

For surface physics experiments, a beam retardation is under work. This system bends e/m resolved beams into the Rossendorf v.d.Graaff beam line, decelerates the ions and can focus them to a grounded target in a UHV chamber. Systematic simulations confirmed, that a four electrode decelerating lens driven by voltages between -0.2 and -0.8 of the acceleration voltage can produce a beam spot of 5 mm diam. corresponding to a target to source magnification of 5/8. If the lens reduces the ion energy to 1/100, the remaining field strength at the target is about 100 V/cm. This field at the target is reduced if deceleration or focusing are less strong. On the base of the technique described here this setup will be employed for sputtering of insulating and semiconducting materials and ion-assisted thin film formation with slow ions carrying high potential energy.

Work supported by Bundesminister für Forschung und Technologie, Sächsisches Staatsministerium für Wissenschaft und Kunst and Volkswagen Stiftung

References

[1] L. Friedrich, E. Huttel, R. Hentschel and H. Tyrroff
Proc. 11. Int. Workshop on ECRIS, Groningen, (1993) 19

[2] I. Steinert, G.D. Shirkov and G. Zschornack
Nucl. Instr. Meth. A 314, (1992) 602

[3] N.A. Tokareva and G.D. Shirkov
Comm. of the Joint Inst. for Nucl. Research, Dubna, P9-93-240, (1993)

[4] K. Bernhardi and K. Wiesemann
Plasma Physics, Vol. 24, 8, (1982) 867

[5] R. Friedlein
to be published

Formation of Double-Height Si(001) Steps by Sputtering with Xe Ions – a Computer Simulation

K.-H. Heinig, D. Stock*, H. Böttger, V.A. Zinovyev**, A.V. Dvurechenskii**, and L.N. Aleksandrov**
*AT&T Bell Laboratories, 600 Mountain Ave, Murray Hill, New Jersey 07974
**Institute of Semiconductor Physics, Novosibirsk, 630090, Russia

Crystal growth on vicinal surfaces is frequently used to study monocrystalline layer deposition by molecular beam epitaxy (MBE). Especially, the temporal profiles of reflection high-energy electron-diffraction (RHEED) specular intensity oscillations measured during MBE of stepped surfaces have shown that there is a strong dependence of the growth mode on temperature. At high temperatures, an approximately constant RHEED intensity results from growth by step propagation (see Fig. 1), whereas at lower temperatures the oscillating RHEED intensity can be explained by two-dimensional nucleation of adatoms forming islands.
Recently a similar behaviour has been found during layer-by-layer sputtering of vicinal silicon surfaces [1]. For ions with sufficiently low energy an atomic layer control in the removal of atoms has been demonstrated. This behaviour has been explained by the production of isolated surface vacancies which are confined to a single atomic layer (Fig. 1). It has been argued [1] that, in analogy to the behaviour of adatoms, the surface vacancies migrate, nucleate to form "vacancy islands", and coalesce to give rise to layer-by-layer removal of the silicon surface.

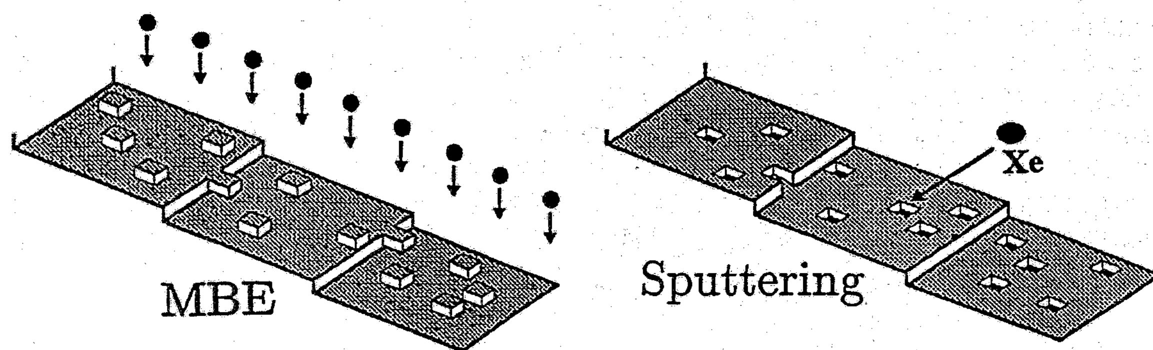

Fig. 1: Scheme of the analogy between growth by MBE and layer-by-layer removal by low-energy ion irradiation which was suggested in ref. [1] and which must be modified in view of our results.

In contrast, recent modeling of layer-by-layer sputtering of Si(111) surfaces has shown that there is no complete analogy with layer-by-layer deposition [2]. By molecular dynamics (MD) calculations it was demonstrated that a single 225 eV Xe ion impact with an angle of incidence of 60° produces on Si(001)-(2 × 1) surfaces no isolated vacancies, but one vacancy cluster, some adatoms and on the average about one sputtered atom (Fig. 2) [3]. In order to determine averages, a series of MD simulations has been carried out for different impact points.

Using the results of the MD simulations as input, the step kinetics on Si(001)-(2 × 1) surfaces was calculated by means of reaction-diffusion equations. On a Si(001)-(2 × 1) surface there are different kinds of steps. As the surface atoms form dimer rows (see Fig. 2), the S_A-steps with dimer rows of surface atoms parallel to the step are different from S_B-steps with dimer rows perpendicular to the step. The kinetics of the steps is determined by adatom diffusion as well as their attachment and detachment at steps and vacancy clusters (Fig. 3).

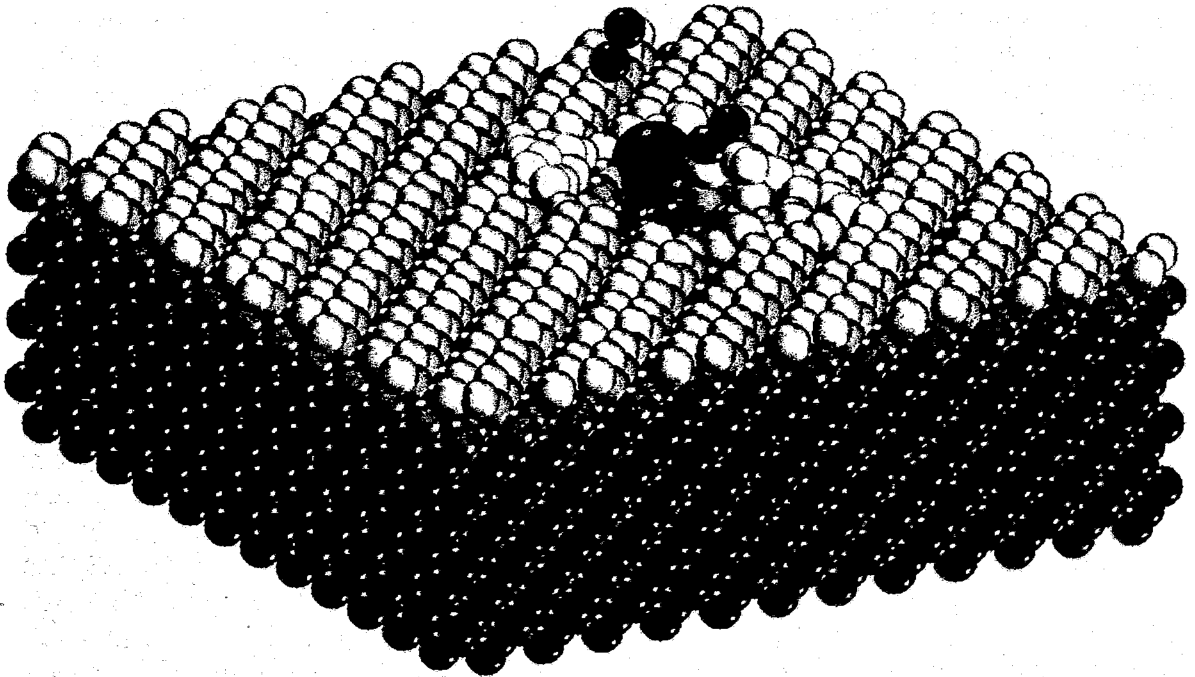

Fig. 2: Surface damage 0.4 ps after a 225 eV Xe ion impact.

The numerical integration of the reaction-diffusion equations confirms the assumption that mobile adatoms control the kinetics of the layer-by-layer sputtering, whereas vacancy clusters are immobile. The calculations give a maximum vacancy cluster concentration near the S_A-steps. The velocity of S_B-steps is about one order of magnitude higher than that of S_A-steps (see Fig. 3), which agrees with experiments [1]. Due to this strong difference in the step velocity double-height Si(001) steps can be found after sputtering of about one monolayer. Additionally, Fig. 3 shows that the velocity difference between S_A- and S_B-steps depends only slightly on the average size of the vacancy clusters.
According to the simulations [2,3] the double-height Si(001) step formation is due to both the detachment energy, which is lower for atoms at S_B-steps, and the difference between the diffusion coefficients of the two terraces.

In summary it can be concluded that, contrary to the suggestion in ref. [1], mobile surface vacancies are not necessary to explain the formation of double-height Si(001) steps. In a consistent manner the mechanism can be described by immobile vacancy clusters, the attachment and detachment of atoms at steps and the diffusion of adatoms across the terraces. A more detailed simulation using Monte-Carlo techniques is in progress.

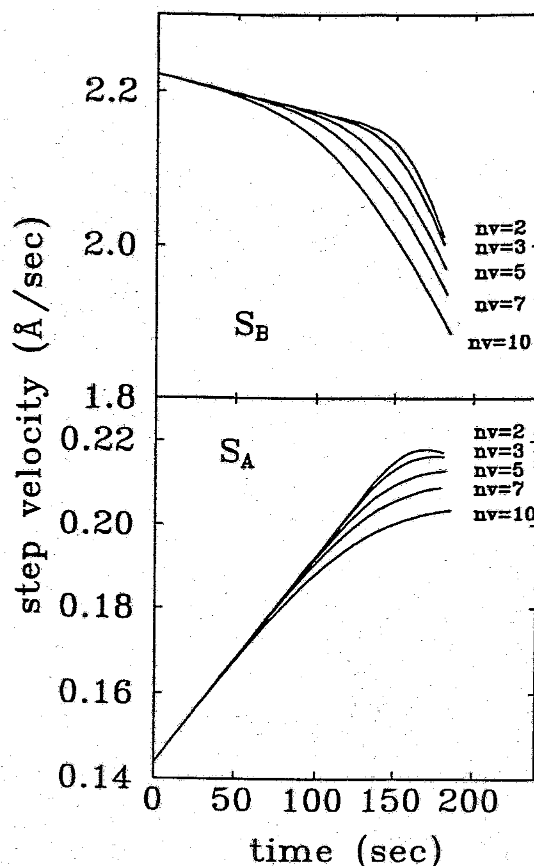

Fig. 3: Velocities of the steps S_B and S_A versus the sputter time for different sizes of vacancy clusters and for a Xe ion intensity of 2×10^{-12} cm^{-2} sec^{-1}.

This work was supported by the Bundesminister für Forschung und Technologie under Grant No. 211-5291-03-HE3ROS.

References

[1] P. Bedrossian, J.E. Houston, J.Y. Tsao, E. Chason, and S.T. Picraux, Phys. Rev. Lett. 67, 124 (1991).
P. Bedrossian and T. Klitsner, Phys. Rev. B, 44, 13783 (1991).
P. Bedrossian and T. Klitsner, Phys. Rev. Lett. 68, 646 (1992).

[2] V.A. Zinovyev, L.N. Aleksandrov, A.V. Dvurechenskii, K.-H. Heinig, and D. Stock, Thin Solid Films, in press (1994).

[3] K.-H. Heinig, D. Stock, H.Boettger, V.A. Zinovyev, A.V. Dvurechenskii, and L.N. Aleksandrov, MRS Proc. vol. 316 (1994).

Self-Organisation During Ostwald Ripening in Ion Beam Synthesis of Buried Compound Layers

S. Reiss and K.-H. Heinig

Ion Beam synthesis of buried oxide (SIMOX) layers has been successfully applied to fabricate silicon-on-insulator (SOI) structures suitable for various advanced microelectronic applications. The synthesis of such layers consists of two technical steps: a high dose implantation step followed by a high temperature annealing step. However, a broad application of this technique is hindered by high costs, which are strongly related to the implantation dose, and by residual defects. Low implantation doses lead to a concentration of the implanted species below that of their chemical compound with the bulk material (substoichiometric doses), and it is more difficult to obtain stoichiometric layers from such substoichiometric doses by annealing. Especially in this case a better theoretical understanding of the layer formation will help to control the process.
The general scheme of the formation of ion beam synthesized compound layers can be considered as consisting of five overlapping stages, namely supersaturation of implanted atoms, nucleation of precipitates of a second phase, growth, Ostwald ripening, and coalescense of these precipitates. More specifically, Ostwald ripening is a process by which, during high temperature annealing, some larger precipitates grow at the expense of smaller ones. The driving force is the minimisation of interface energy, which leads to a radius-dependent equilibrium concentration c_G for every precipitate, given by the Gibbs-Thomson-equation. This process plays a key role in the segregation of the implanted atoms resulting eventually in the formation of a buried layer.
Existing theories of Ostwald ripening are only asymptotic descripitions of homogeneous systems of precipitates. In the present work, a theoretical model and a simulation program were developed for the ripening of a spatially inhomogeneous system like a layer of precipitates in a substrate[1-4]. In a first step a large but finite ensemble of precipitates was chosen, as a mathematical problem of a divergence arises for a system with an infinite number of precipitates and even for a finite system with periodical boundary conditions. For the same reason, the experimental geometry of a layer beneath a surface was simulated by a shell of precipitates surrounding a huge central precipitate simulating the surface.
Contrary to the ripening of spatially homogeneously distributed precipitates, where the scaled radius distribution in the limit $t \rightarrow \infty$ becomes independent of the initial distribution, the initial and boundary conditions have a crucial influence on the evolution of the ripening in a spatially inhomogeneous ensemble. Experimental studies of the initial stage for the ripening show that to a first approximation all precipitates exhibit the same size and are homogeneously distributed in the layer. This result has been used for the simulation (Fig. 1a). The boundary condition of the concentration field in infinite distance was set to the solidus of oxygen in silicon c_∞.

To take all collective effects into account the whole interaction matrix has to be considered. Thus, the computer simulation of Ostwald ripening requires the numerical integration of thousands of strongly coupled reaction-diffusion equations, which describe the growth and/or the dissolution of precipitates.

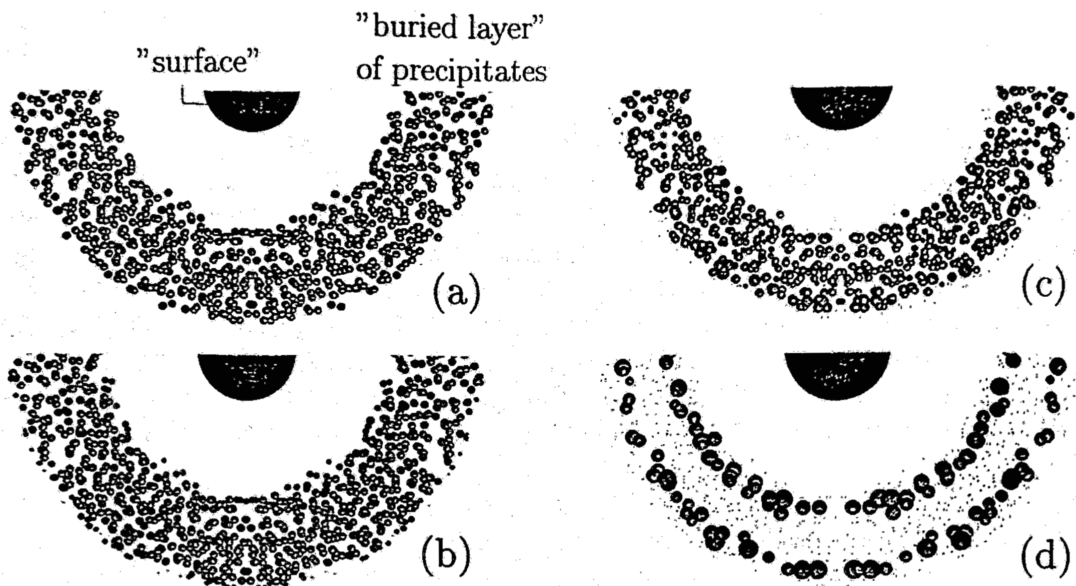

Figure 1: Cross section through the ensemble at beginning and the end of the simulation. Only one half of the ensemble is shown.
(a) initial stage: Simulating nucleation, 6704 precipitates with an initial radius of 10 nm are randomly placed in a 240 nm thick shell at 240 nm distance from the "surface" (the huge central precipitate), thereby taking into account that nucleation in a "halo" surrounding existing precipitates is forbidden.
(b) dissolution at the periphery: After some time, at the inner and at the outer periphery of the "buried layer" precipitates become smaller (dissolution).
(c) precipitate grow in the next inner region: At a later time, two layers of growing precipitates begin to form.
(d) result of the simulation: From the initial distribution a two band structure of precipitates evolved. This structure is similar to that found experimentally by [5].

The calculations show that a finite ensemble of spherical precipitates is able to form a structure of shells of growing and vanishing precipitates. The distance between these shells, which we call "structure wavelength", increases with decreasing initial volume fraction of the precipitates. In Fig. 1d two shells of large precipitates have developed, a case which has been observed experimentally by different groups[5]. Less (one) ore more shells (layers) have been found by our modeling as well as experimentally (e.g. the "banding"[6]) too. The scheme of the underlying physics is shown in Fig. 2.

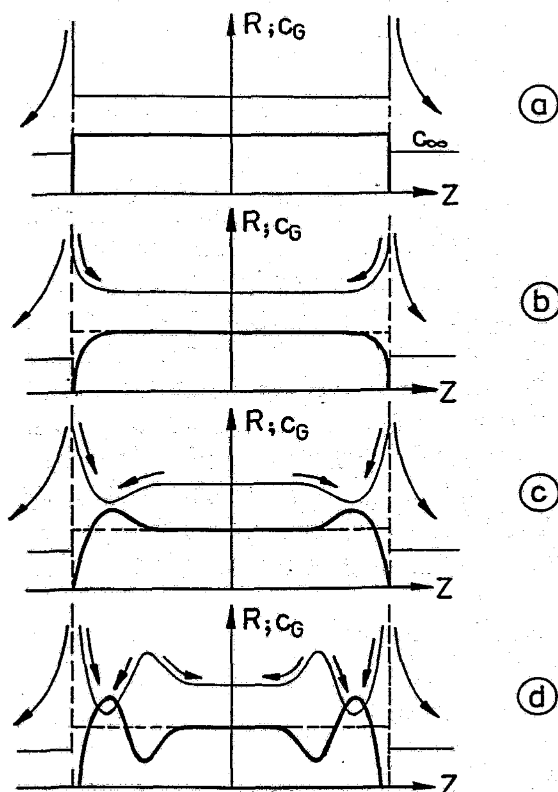

Figure 2: Scheme of structure formation – a self-organisation.
(a) initial stage: Precipitates with equal radius (thick line) and, therefore, equal c_G (thin line) are homogeneously distributed in the layer.
(b) dissolution at the periphery: Due to the lower concentration level c_∞ in the bulk and at the surface, the outermost precipitates lose oxygen by diffusion, their radii shrink and their c_G grow. Oxygen diffuses outwards and inwards.
(c) evolution of two peaks: The nearest inner precipitates grow and lower their c_G. Now, oxygen diffuses from outside and then also from inside to these growing precipitates.
(d) propagation of structure: Smaller precipitates develop inside of this layer of growing precipitates. Due to their higher c_G, oxygen diffusion starts to the next inner region – the structure formation propagates!

In summary, we found that in a buried layer of equal-sized precipitates a self-organisation takes place. This self-organisation explains for the first time in a simple and consistent manner structures like "humps", "spikes" and "banding" found experimentally. The number of bands of precipitates depends on the initial volume fraction of the precipitated material.

This work was supported in part by the Bundesminister fuer Forschung und Technologie under grant no. 211-5291-03-HEROS. We thank Mr. Horst Boettger for visualising the data.

References:

[1] S. Reiss and K.-H. Heinig, E-MRS 1993 Spring Meeting, Strasbourg (France), May 4.-7., 1993, contrib G-VI.11. and Nucl. Instr. & Meth. B 84/2 (1994) 229
[2] S. Reiss, R. Weber, K.-H. Heinig, and W. Skorupa, ECAART 93, Orleans (France) and Nucl. Instr. & Meth. B (1994), in press
[3] R. Weber, R. Yankow, R. Mueller, W. Skorupa, S. Reiss, and K.-H. Heinig, MRS Proc. vol. 316 (1994), in press
[4] S. Reiss, K.-H. Heinig, R. Weber, and W. Skorupa, MRS Proc. vol. 316 (1994), in press
[5] P. L. F. Hemment, K. J. Reason, J. A. Kilner, R. J. Chater, C. Marsh, G. R. Booker, G. K. Celler, and J. Stoemenos, Vacuum 36 (1986) 877
[6] S. Nakashima and K. Izumi, J. Mater. Res. 8 (1993) 523

Modification of Metals and Other Materials

H. Reuther

High dose implantation of Al and Si into iron studied by Mössbauer spectroscopy

Iron samples were implanted with 5 x 10^{17} cm^{-2} Al ions at an energy of 50 keV and a current density of 3,7 $\mu A/cm^{-2}$. Different FeAl phases were formed in dependance of the thermal conditions. Depth-selective conversion electron Mössbauer spectroscopy was applied to determine the depth in which the phases were formed. A layer structure was obtained with an uppermost non-magnetic and a subsequent magnetic FeAl phase followed by the bulk material α-Fe. Integral conversion electron Mössbauer spectroscopy was used to investigate iron samples implanted with Si. High dose implantation (5 x 10^{17} cm^{-2}, 100 keV and 1 x 10^{18} cm^{-2}, 200 keV, respectively) resulted in the formation of non-magnetic FeSi phases while at lower doses and energies only magnetic phases were formed.

Supported by DFG

Collabration: Universität Duisburg

A. Kolitsch

Ion beam assisted deposition

Amorphous carbon layers were prepared by ion beam assisted deposition and modified by ion implantation. The best films with the highest hardness and Young's modulus were prepared in the energy range between 200 and 600 eV of the assisting Ar^+ ions, with a ion/atom ratio > 1 during deposition and by deposition rates < 5 nm/min. The Raman spectra of the films show two broad bands as known from sp^2-rich amorphous carbon phases. Post-deposition bombardment with 20 keV carbon ions modifies the mechanical properties in relation to the ion fluence. Low fluences up to 10^{16} C^+/cm^2 decrease the hardness drastically. With increasing fluences up to 10^{18} C^+/cm^2 the hardness rises again.

Supported by SMWK

E. Richter

Improvement of adhesion of deposited layers on metallic and polymer materials by ion beam induced mixing (IBM)

The adhesion of aluminium layers on magnesium alloys (Mg9Al) was improved by IBM by a factor about 2 - 4. The magnesium alloys deposited with aluminium were bombarded with Ar^+ ions with an energy of 150 keV (penetration depth is similar the thickness of the Al films) and a fluence of 1.5 x 10^{16} Ar^+ cm^2. At the same conditions similar results were found for layers of aluminium, chromium and copper on different polymer substrates (Piacryll, PTFE).

R. Günzel
J. Brutscher

Construcion and test of a plasma source ion implantation (PSII) facility

The construction of a facility with a 15 l chamber using a plasma generated by a filament assisted DC discharge has been completed. A pulsed voltage with a maximum of 75 kV could be achieved. The time for implantation of 10^{17} oxygen or nitrogen ions/cm^2 was about 20 minutes. The profiles of the implanted ions were measured by AES. PSII of nitrogen yields a depth profile similar to beam line implantations, whereas after PSII of oxygen the resulting oxygen profile was strongly dominated by oxygen indiffusion into the bulk from residual gas.

R. Küchler

Characterization of residual stress in the near surface region with surface acoustic waves

The influence of the residual stress in TiN coatings on the velocity of acoustic waves was investigated by means of sing around method. The measured velocity can be used to determine the elastic modulus or the residual stress of a film. For that, knowledges of the materials parameters of substrate and the film thickness are necessary. The elastic modulus in dependence of the residual stress was determined. Therefore, the stress in the layers was evaluated from the curvature of the bended sample. For that, thin plates were sawn off the coated samples with a diamond wire. For example, it has been found that a compressive residual stress of 4 GPa in the layer causes a velocity change about 15 %. The error in the determination of Young's modulus by this velocity change amounts to about 10 % if the error of film stress is negleted.

Supported by DFG

H. Reuther
J. Steffen

Investigations of surfaces modified by ion beams by means of AES and XPS

Since April 1993 a new MICROLAB 310 F (FISONS Instruments) has been available. The MICROLAB 310 F is a scanning Auger spectrometer with field emission electron source and hemispherical sector analyser and with XPS facility. After testing it was used mainly to determine elemental depth profiles produced by ion implantation (for instance, Al and Si in Fe, O in Al and Mg, C in Si) and to check the homogenity of deposited layers (Ta oxide on Si).

M. Seidel

Measurement of friction and wear of ion beam modified metallic materials

A new equipment for investigations of the friction coefficient and the wear behaviour was constructed and tested. It allows measurements by the pin-on-disk and the ring-disk technique. A PC is used for controlling and analysis.

Modification of Semiconductors and Patterning by Focused Ion Beam

R. Weber
R. Yankov
R. Müller
W. Skorupa

Experimental study of precipitation processes in oxygen-implanted silicon

For the purpose of SIMOX (Separation by IMplanted OXygen) modeling, precipitation studies were performed in silicon after high dose oxygen implantation and high temperature annealing. Results obtained by XTEM gave evidence that Ostwald ripening in the oxygen-rich silicon starts from silicon oxide precipitates which are of comparable size and homogeneously distributed throughout a substoichiometric buried layer. With increasing annealing temperature, a clear trend of the SiO_2 precipitates to arrange in well defined regions was revealed. An inherent process of self organization, as distinct from earlier claims concerning ion beam induced nucleation enhancement, is indicated.

Supported by BMFT

N. Hatzopoulos
*D. Siapkas**
PLF Hemment[+]
W. Skorupa

Formation and Characterization of double SIMOX structures

Novel buried double-layered SIMOX structures have been produced by the sequential high and low energy implantation of oxygen into silicon at 2 MeV and 90 keV. Each implantation step was followed by high temperature annealing. Infrared reflection spectra of the samples were analyzed and results were compared to those of RBS. No interaction or transport of oxygen between the two layers was evidenced. Both the in-between silicon layer and the top Si overlayer are of high crystal quality. All the Si-SiO_2 interfaces are found to be quite sharp and so, one of the basic conditions for high quality optical waveguiding is met.

Collaboration: University of Thessaloniki, Greece (*); University of Surrey, UK (+)

R. Kögler
J. von Borany
D. Panknin
W. Skorupa

Electrical Effects of Residual Defects in Si after High Energy Implantation of Ge^+ Ions and Annealing

Electrical effects of residual defects after high energy implantation of Ge^+ ions and high temperature annealing were investigated. The results show a remaining reduced carrier concentration in the full depth range between the surface and the mean projected Range R_P. The reverse current of high energy implanted diodes was significantly reduced for Ge doses below the amorphization level. The reverse current is enhanced, however, when doses are high enough to form a buried amorphous zone. This effect is caused by generation centers which were found to be located inside the regions of "end of range"-defects joining the amorphous layer.

Supported by BMFT

V. Heera
R. Kögler
W. Skorupa
*E. Glaser**

Ion beam induced epitaxial crystallization of single crystalline 6H-SiC

For the first time, ion beam induced epitaxial crystallization (IBIEC) of SiC has been found and investigated by RBS/C and XTEM. An amorphous surface layer was produced by 200 keV Ge^+ implantation into single crystalline 6H-SiC. A shrinkage of the amorphous layer by 57 nm (300 keV) was found after irradiation with $3 \cdot 10^{17}$ Si^+/cm^2 at 480°C which is about 1000°C below the threshold temperature for thermally induced solid phase epitaxy (SPE) of this wide band gap semiconductor material. It is caused by both an initial thermal regrowth and ion beam induced epitaxial crystallization. However, the initial thermal regrowth stops after 20 nm and can't be continued below 1450°C, whereas the recrystallization proceeds under ion irradiation with a rate of about 1.5 nm/ 10^{16} cm^{-2}.

Supported by DFG

Collaboration: Institut für Festkörperphysik der FSU Jena (*)

D. Panknin
*W. Henrion**
E. Wieser
M. Voelskow
W. Skorupa

Structural and optical properties of Co alloyed β-$FeSi_2$ formed by ion beam synthesis

The investigation of ion beam synthesis of semiconducting silicides by high dose implantation of 3 d metals in Si shows the possibility of changing the band gap energy. For this purpose ion beam synthesized $FeSi_2$ was alloyed with cobalt by ion implantation. The microstructure was investigated by RBS and TEM. The band gap energy was determined by Infrared Spectroscopy. With increasing Co concentration the band gap energy decreases from 0.84 eV for pure β-$FeSi_2$ to 0.68 eV after replacements of 15 % of the iron atoms by Co. The shift of the band gap is due to the formation of band tail states and, especially for high Co concentration, by the influence of lattice distortions on the band gap.

Collaboration: Hahn-Meitner-Institute, Berlin (*)

J. Teichert
L. Bischoff
E. Hesse
W. Skorupa
D. Panknin

Formation of $CoSi_2$ wires by maskless implantation with a focused ion beam

The maskless ion implantation with the focused ion beam was used as a new method for ion beam synthesis of cobalt silicide wires is presented. In order to perform the implantation a special achromatic mass seperator was implemented into the ion column. Ion implantation was performed with 30 keV Co^+ and 60 keV Co^{++} ions. The dose dependence for room temperature implantation and the influence of the substrate temperature were investigated. This alternative method of writing a beam with a very small spot size should be of considerable interest for the fabrication of submicron structures. The results obtained up to now confirm the physical equivalence of broad beam and focused ion beam implantation.

Supported by BMFT

L. Bischoff
J. Teichert
E. Hesse
*T. Geßner**
*Löbner**

Application of the Focused Ion Beam for the fabrication of micromechanical devices

The advantages of the Focused Ion Beam and micromechanical technology were combined in order to form structures which cannot be obtained by other techniques, such as a micropattern on the bottom of an etched groove, and conducting paths betweeen the lower and upper level of such agroove should be investigated. Also the fine tuning of resonance devices and the sputtering as a alternative method to the wet chemical etching are examples of the project activities. First experimental results were obtained in the field of sputter etching as well as first conducting pathes ($CoSi_2$ - wires) were written on silicon.

Supported by SMWK

Collaboration: Technische Universität Chemnitz-Zwickau (*)

E. Hesse
L. Bischoff
J. Teichert

Development of cobalt containing liquid alloy ion sources

Two types of cobalt containing liquid metal ion sources were developed and investigated to its suitability for focused ion beam implantation. From the metallurgic point of view with respect to a relatively low operation temperature a Nd-Co composition was chosen. The melting temperature in the eutectic point amounts to 566°C at a cobalt concentration of 36 atomic percent. A problem of using neodymium is its high reactivity to oxygen. This oxidation during the transfer of the emitter from the vacuum chamber, used for preparation, to the focused ion beam system can be reduced by a protective cover of benzine and a minimized handling time. The relatively high fraction of doubly charged cobalt ions allows to use them for implantation and expands the energy range.

E. Hesse
F.K. Naehring
J. Teichert

A lithium liquid metal ion source with narrow angle emission for writing beam lithography

The current-voltage characteristics and the ion current fluctuations of a lithium liquid metal ion source have been determined. The angular intensity has been measured in dependence on the emission angle and on the ion current. The high angular intensity and the large range of light ions suggest the liquid metal ion source to be applied for writing beam lithography. PMMA resist layers were exposed by a focused lithium ion beam.

L. Bischoff
J. Teichert
G. Hofmann
W. Probst
J.E. Wagenaar

Improvement of the FIB equipment IMSA - 100

A digital scan and image processing system including the software were developed and implemented. To use the beam blanker for aligment purposes a special fast switch control modul was built. For the writing implantation application of the FIB a high resolution double E x B mass separation system was built an introduced into the ion optical column. To expand the application possibilities of the FIB (ion beam synthesis, in-situ measurements etc.) a sample handling system including a wafer heater up to 500° C was implemented in the target chamber.

Th. Henkel
V. Heera
R. Kögler

Development and test of an optical in-situ technique for time resolved reflectivity measurements

An optical in-situ technique for time resolved reflectivity measurements (TRR) has been installed at the tandem accelerator. This technique is a powerful and flexibel tool for the investigation of ion beam induced epitaxial crystallization (IBIEC), planar amorphization (IBIIA) as well as ion beam induced damage in semiconductors. Application of our TRR system to an IBIEC-experiment in silicon shows, that the velocity of the amorph-crystalline interface remains constant within the bulk and decreases near the surface.

Supported by
DFG, BMFT

Application of Ion Beams to Sensors

(A) Chemical Microsensors

M. T. Pham
J. Hüller

Coupling of Silver Halogenides to Field Effect Dielectric Layers: Incorporation of AgJ into Thin Films of SiO_2

Implantation of Ag^+ and J^+ ions into thin SiO_2-layers have been studied to realize ion sensing membranes for field effect microsensors to detecting Cl^-, Br^-, J^-, Cn^- and Ag^+ ions. Auger electron spectra reveal the presence of AgJ after implanting Ag^+ and J^+ to concentrations greater than $1x10^{21}cm^{-3}$ followed by a thermal treatment at temperatures ranging from 600 to 900 °C. The measured sensitivity to Cl^- ions in an electrolyte was explained by the formation of the AgJ-phase in the SiO_2 matrix.

Collaboration: Institut Fresenius für Angewandte Festkörperanalytik GmbH Dresden

M. T. Pham
S. Howitz

Sodium Aluminiumsilicate Thin Films (NAS) with Ion Beam Controlled Compositions studied by Auger Spectroscopy

Submicron films of NAS were fabricated by implanting Na^+ and Al^+ into CVD-SiO_2. Auger Spectroscopy has been employed to analyze the chemical state of the film constituents and the chemical composition depth profile. From the measured Auger spectra the conversion of SiO_2 into silicate can be explained as follows: a) incorporation of Al into the SiO_2-network, b) reaction of the Na- and Al-components with oxygen from the SiO_2-matrix, c) appearence of Si-valence states smaller than 4, and d) depletion of bridging oxygen at the end of the implantation trajectories. The ion sensitivity of the NAS thin films was verified in dependence on the surface Al/Na-concentration ratio of the implanted layers.

Collaboration: Institut Fresenius für Angewandte Festkörperanalytik GmbH Dresden

J. Hüller
M. T. Pham
S. Howitz

Ion-Beam Synthesis of Thin Chalcogenide Films: Formation of Buried Arsenic Selenide in SiO_2

Bulk materials of chalcogenides are utilized as sensing membranes for heavy metal ions in electrolyte so far. Thin film materials required for use in microsensors have been studied by implanting As^+ and Se^+ into SiO_2. Arsenic selenide layers buried in SiO_2 formed by the reaction between As and Se after implantation and thermal treatment were identified from Auger electron spectra analysis. The sensitivity to Cu^{2+} ions of the implanted layers has been investigated using EIS measurements (Electrolyte Insulator Semiconductor) and was attributed to the identified arsenic selenide.

Supported by AiF

Collaboration: Institut Fresenius für Angewandte Festkörperanalytik GmbH Dresden and University St. Petersburg

M. T. Pham
S. Howitz
M. Bürger
U. Müller
*T. Wegener**

Chemical Sensor with Membrane Array of Graduated Ion-Mixed Sensitivity

An array of ISFETs (Ion-Sensitive Field Effect Transistor) and EIS capacitors (Electrolyte Insulator Semiconductor) with a sensitivity gradient (to Na^+, K^+, H^+) based on gradually varying membrane compositions (xNa_2O. yAl_2O_3. $zSiO_2$) has been prepared by ion implantation. The simultaneous multiion detection with such an array is being studied using the chemometric evaluation for pattern recognition.
Collaboration: TU Dresden (*)

S. Howitz
M. T. Pham
M. Bürger
H. Fiehn
A. Steinbach
T. Vopel

Supported by SMWA

Development of a Fluidic ISFET Microsystem (FIM)

Results in 1993 concerned to all major system components: a) measurement electronics, b) ISFET-microsensors, c) microactuators (pumps and valves) and d) fluidic microcells and microchannels, as well as wafer processing for micro-packaging and interconnections. After manual assemlage of all components to a complete microsystem prototype, the system functionality is being studied in test measurements.
Collaboration: Zentrum Mikroelektronik Dresden GmbH, FhG-IMS 2 Dresden, Institut Fresenius für Angewandte Festkörperanalytik GmbH Dresden

T. Vopel
S. Howitz
M. Bürger
M. T. Pham

Supported by SMWA

Micro Flow Injection Measurements (FIA) Using Components of the Fluidic ISFET Microsystem (FIM)

Dynamic differential measurements for multiion detection were performed with an electrochemical detector module for FIA including ISFET-microsen-sors arranged in a micro-multichannel system of the FIM-fluidic microcell. Results obtained with pH-ISFETs have been evaluated concerning accuracy, reproducibility and capability of the fluid handling to meet requirements for analysis in environmental applications. Extension to a module for simultaneuos multicomponent detection (pH, pNa, pNO_3) in soil analysis is being in progress.
Collaboration: Institut Medizintechnik GmbH Dresden

H. Fiehn
S. Howitz

Supported by SMWA

Simulation of the fluid transport in microchannel systems

Numerical calculations based on the finite element method (FEM) are carried out to simulate the fluid motion in microchannel systems used in the fluidic ISFET microsystem (FIM). Aim of the study is to optimize the design and fabrication cycles of the micromachined device components and to get an insight into processes involved in the micro-fluid handling not readily accessible to experiments. Results obtained so far refer to the description of the fluid flow conditions in an ISFET microcell, and predict an optimal shape geometry of the device for suppressing whirls and turbulances in fluid chambers of micropumps and valves.

(B) Radiation Detectors

I. Beatus
B. Schmidt

Photoresist Masking for MeV-Ion Implantation

For masking high energy ion implants modified AZ1350H photoresist with a high specific weight of 1.1022 g/ml and 1.1125 g/ml has been used. The resist was spinned on the wafers using low a rotation velocity of 1500 rpm to achieve a homogeneous layer thickness up to 50 µm. Applying double resist exposition and development an edge slope of the pattern in the range from 0.5 up to 0.6 has been observed for layer thicknesseses of 15 µm and 50 µm respectively. 15 µm thick and lithographically patterned resists have been succesfully applied to masking 6 and 10 MeV phosphorus implants in the silicon radiation detector fabrication process.

J. von Borany
B. Schmidt

Silicon pn-Junction Detectors with Built-in High Field Region

High energy phosphorus implantation has been used to realize $p^+nn^{(+)}nn^+$-silicon detector structures. Applying P^+-MeV-implantation to buried $n^{(+)}$-layer formation a constant electric field strength $\geq 10^5$ V/cm up to a depth of some µm from the detector surface can be achieved. Buried $n^{(+)}$-layers were implanted with P^+-ions at E = 6 and 10 MeV and D = 10^{11} and 10^{12} cm^{-2} and annealed at 900 °C for 30 min. From the measured C-V-characteristics the depth of the high field region and the implantation profiles have been determined. The I-U-characteristics show low detector reverse currents of $I_r \approx (30...50)$ nA (at bias $U_r = 100$ V). Detectors with built-in high electric fields can be advantageously used in heavy ion and fission fragment spectroscopy.

B. Schmidt
*V. Eremin**
*A. Ivanov**
*N.Strokan**
*E. Verbitskaya**
Z. Li[+]

Relaxation of Radiation Defects in Silicon Detectors

The behaviour of radiation induced carbon related defects in high resistivity silicon detectors has been investigated. The defects were introduced by α-particle irradiation and the measurements were carried out using the DLTS-technique. The unusual defect behaviour consists in low temperature annealing, including self annealing at room temperature, of the interstitial carbon C_i with a simultaneous increase of the $(C_i\text{-}O_i)$-complex concentration. The kinetic parameters of the process have been determined from the increase of the C_i-centre concentration versus time. Two annealing velocities have been observed, which are due to different heat treatments during the detector fabrication process.

Supported by BMFT

Collaboration: FZR Rossendorf, PTI St. Petersburg (*), NBL Brookhaven (+)

B. Schmidt
J. von Borany

Preparation and Characterization of Ultra Thin Silicon Membranes

The electrochemical etch stop behaviour of ion-implanted n-type layers has been investigated. A three-electrode potentiostatic configuration and a KOH/H_2O etch solution were used for these studies. Energy-loss spectro-metry of α-particles was applied to measure the absolute membrane thick- ness with an accuracy of ±3.5%. The smallest membrane thickness has been measured as (1.15...1.45) µm. The thickness investigation shows that the etch stop takes place (1.0...1.2) µm before the implanted metallurgical p-n junction is reached. From profile and electric field calculations it was concluded that the difference between the measured membrane thickness and the pn-junction depth is caused by the depletion layer in the p-substrate. Additional HNA isotropic etching was carried out to reduce the membrane thickness to 300 nm.

J von Borany
J. Goerigk
W. Voitus

Fully Ion-Implanted HP-Ge-Detectors for EUROBALL

Phosphorus implanted layers on high purity germanium have been investigated to replace Li-diffused n^+-contacts for planar HP-Ge-detecors. Implantation and annealing parameters were optimized concerning electrical dopand activation and stability of substrate net doping ($N \sim 10^{10}$ cm^{-3}). XPS-investigations result in a pre-implantation hydrochloric acid based treatment to avoid germanium oxide and oxygen recoil implantation. A fully electrical activation for P^+, 50 keV, $5x10^{14}$ cm^{-2} is realized by a flash lamp annealing (t_p=20 ms) at 700°C, resulting in sheet resistivities around 50 Ω/□. Fully ion implanted diodes ($A=14mm^2$) with reverse currents of some pA and breakdown voltages above full depletion have been achieved.

Supported by
BMFT

Collaboration: GSI Darmstadt, CRN Strasbourg, INTERTECHNIQUE Strasbourg

Ion Beam Analysis, Fundamentals of Ion-Solid-Interaction and Accelerator Technique

R. Grötzschel
M. Mäder

Supported by
BMFT
SMWK

Ion beam analysis of silicide and HTSC layers
The composition of thin layers of transition metal silicides and of high temperatur superconductors was determined with RBS using 1.2 - 1.7 MeV 4-He ions or 16-O ions with energies between 15 and 25 MeV. The layers had been deposited by various methods or by ion beam synthesis. By He ion channeling the epitaxial or mesotaxial growth and the obtained crystalline structure was characterized.
Collaboration: Technische Universität Chemnitz-Zwickau, Universität München

D. Grambole
F. Herrmann

Nuclear resonance depth profiling of hydrogen
Measurements of hydrogen depth profiles or concentrations in thin layers of silicon oxinitride, carbon, amorphous germanium and metals were performed using 15-N ions at the tandem accelerator. To achieve a homogenous irradiation at variable spot sizes a scanning system, consisting of an electrostatic scanner, a cross collimator and a quadrupole lens was installed.
Collaboration: Universität Frankfurt/M., Technische Universität Chemnitz-Zwickau, Technische Universität Dresden

U. Kreißig
R. Grötzschel
*R. Behrisch**
S. Grigull

Simultaneous light element analysis by HIERD
The parallel operation of a solid state detector telescope and a Bragg ionization chamber allows the simultaneous analysis of all elements with $Z < 12$ by recoil spectrometry using heavy ion incidence (HIERD). The depth profiles of the hydrogen isotopes and light elements up to oxygen were studied in surfaces of plasma exposed wall material from fusion machines.
Collaboration: IPP Garching (*), Beschleunigerlaboratorium der Universitäten München

W. Jiang
R. Grötzschel
K. Schulze

Stopping cross sections and charge exchange of channeled MeV ions
The beamline and the scattering chamber at the tandem accelerator were set up. A transmission channeling goniometer and a beam deflection system for ultralow beam current mesurement is under construction.

D. Grambole
F. Herrmann
C. Neelmeijer
W. Wagner

PIXE analyses of thin films and surface layers

PIXE at the tandem accelerator was used to measure the contaminant concentration in sputtered Ge films and in steel samples from nuclear reactor material. The element concentration ratios of As and Se in silicon oxinitride structures and of Fe and S in pyrites was studied by PIXE. In combination with the nuclear microprobe, trace element mapping in microscopically small granite crystal grains was performed.

Collaboration: HMI Berlin, Universität Göttingen, Universität Greifswald

C. Neelmeijer
W. Wagner
*H.-P. Schramm**

Supported by BMFT

Paint layer studies using PIXE on air

Pigment combinations (verdigris/white lead or chromium oxide/zinc white) arrange both as double paint layers and two component admixtures were prepared and analyzed by PIXE at the external proton beam of AGLAE (Louvre Laboratory, Paris). Variation of the incident proton energy made it possible to deduce the actual layer configuration directly from the x-ray spectra. The GUPIX program served for the calculation of the relative element concentrations.

Collaboration: Hochschule für Bildende Künste, Dresden (*), Laboratoire de Recherche des Musees de France, Louvre, Paris

I. Sandner
M. Büschel
*A. Steuerlein**

Supported by BMFT

Study of sketches on paintings using the computer assisted infrared reflectography

Infrared reflectography represents a powerful tool to image the black sketches under the pigment layers of oil paintings. A computer assisted image processing line has been implemented for acquisition, storage, correction and linkage of single records. Sketches of paintings of Lucas Cranach's workshop have been studied by the infrared method to get informations on their authenticity.

Collaboration: Hochschule für Bildende Künste, Dresden (*), Institut für Farbenchemie der Akademie der Bildenden Künste, Wien

M. Friedrich
S. Turuc
W. Bürger

Supported by BMFT, KAI

Operation and development of the electrostatic accelerators

The 2 MV VdG and the 5 MV tandem accelerators have been operated mainly for experiments in ion beam analysis. The beam stability of the 2 MV VdG accelerator has been remarkably increased using a non-inclined field accelerator tube with magnetic suppression of secondary electrons. The 3 MV HVEE Tandetron was installed and put into operation.

M. Friedrich
W. Bürger
R. Grötzschel
G. Sun
G. Schade

Accelerator mass spectrometry (AMS)

The installation of a special beam line for AMS and energy loss measurements has been started. An improved Bragg ionization chamber for particle detection has been built up. The isotope switching of the deflecting magnets using a PC was realized as a first step to the computer controlled accelerator operation.

Collaboration: TU Bergakademie Freiberg

D. Henke

High energy implantation of ^{7}Be

Searching for conditions of maximum ^{7}BeX- ion source efficiency and operation stability the sputter ion source MISS 790 was tested and optimized with respect to cathode lifetime, current yield and target handling for ^{9}Be and ^{7}Li. Very stable operation is possible using a H_2/O_2 gas cathode. The transmission of the injector assembly has been increased by inserting a double focusing injector magnet. The ion charge distribution after the accelerator has been measured.

Supported by
KfK Karlsruhe/TT

Collaboration: KfK Karlsruhe

H. Tyrroff
D. Henke
*R. Friedlein**
*S. Herpich**
*H. Hiller**
*G. Zschornack**

ECR ion source (Joint project FZR - TUD)

Optimum operational parameters of the 7.25 GHz source in order to obtain high ionic charge states for N, O, Ar, Kr and Xe were identified. Beam handling and retardation optics have been calculated and are under design and construction. Bremsstrahlung spectra and first characteristic X-ray spectra for Ar and Xe were measured using a HPGe detector. A method to obtain the plasma electron energy distribution from Bremsstrahlung spectra has been developed and tested.

Supported by
BMFT, SMWK
VW-Stiftung

Collaboration: TU Dresden (*), Strahlenzentrum Universität Giessen, Universität Frankfurt

M. Betzl
K. Walther
K. Ullemeyer
J. Heinitz

Texture Investigation of Geological Materials by Time-of-Flight Neutron Diffraction

The neutronographic texture investigations of more than 100 geological samples of different type (quartz, carbonate, granulite, amphiobolite, olivine, dolomite, pyrrhotine) were performed in cooperation with 5 national and 2 foreign institutions using the texture diffractometer at the IBR-II reactor in Dubna (Russia). The main topics were: (i) Texture characterizations of rocks with the aim to correlate the texture data with models of genesis of geological formations. (ii) Comparison of the texture of artificially and naturally deformed samples in order to prove models for geological deformation mechanisms. (iii) Characterization of the texture of samples from deep drilling projects (KTB Windisch-Eschenbach, Kola).

Methodic work was undertaken to modernize the spectrometer control system and the data handling software in connection with the introduction of VME computers. The construction of two pressure cells for in-situ investigations of deformation and phase transitions is in progress.

supported by BMFT

Collaboration: Universität Göttingen, RWTH Aachen, TU Clausthal-Zellerfeld, GeoForschungsZentrum Potsdam, TU Dresden, University Aarhus, University of California Berkeley

M. Betzl
Ch. Scheffzük

Texture Investigations on Salinar Rocks from Salt Deposits in Middle Germany

The neutronographic texture investigations on halite were continued. Selected samples from the deposits Zielitz (clod of Calförde) and Merkers (Werra region) were analysed. The main topic was the influence of lithostatic pressure and of intrusions of basalt on the texture of halite. All samples from the Zielitz deposit have a (100) fibre texture, probably due to recrystallization. In contrast, the samples from the Merkers deposit show a (110) fibre texture which can be interpreted as the final stage of a deformation texture after compression.

The neutron experiments were performed at the texture diffractometer of the IIM at the Rez reactor (Czech Republic).

supported by BMFT, SMWK

Collaboration: GeoForschungsZentrum Potsdam

A. Mücklich

Neutronographic Study of the Texture of Metals and Semiconductors

(a) Orientation-dependent grain size determinations were carried out by neutron diffraction at the Rez reactor. In contrast to conventional metallography the method gives information on the real volume of

the grains separately for each texture component. This is a significant step towards a simultaneous analysis of structure and texture. The methodological aim was to develop an evaluation method based on spline interpolation of pole figures.
(b) Polycrystalline silicon which is used for solar energy devices was investigated since the performance of the material significantly depends on both the defect structure and the texture. For obtaining reliable results on bulk samples the neutron diffraction technique has no competition.

supported by SMWK

Collaboration: (a) TU Bergakademie Freiberg, (b) Institut für Kristallzüchtung Berlin, Institute of Nuclear Physics Rez (near Prague)

F. Eichhorn
A. Hempel

Small Angle Scattering Investigations on Materials

The mesostructure of hydrating and hydrated Portland cement paste (type PZ 1-40A) was investigated by neutron small angle scattering in cooperation with the Lab of Neutron Physics in Dubna. In dependence on the hydration time a fractal-like structure was found. This result was confirmed by scanning electron microscopy.
Measurements of the anomalous X-ray scattering on reactor pressure vessel steels (Soviet type 15Kh2MFA) were started at HASYLAB. Using the contrast variation method near the absorption edges it seems that vanadium rich precipitates were formed during the neutron irradiation. The investigation is part of a program to study neutron embrittlement of reactor pressure vessel steels,in cooperation with the Institute of Safety Research of the FZR.
The installation of the double crystal neutron diffractometer with perfect crystals at the reactor BER-II at the HMI Berlin started in September 1993. The instrument uses a completly asymmetric analyzer and a linear position sensitive detector. The exploitation will start in 1994.

supported by BMFT

Collaboration: Frank-Laboratory of Neutron Physics at JINR Dubna (Russia), Institute of Safety Research at FZR, HMI Berlin, Technische Fachhochschule Berlin

F. Prokert

Phase Transitions in Ferroelectric Crystals

The investigations of the low temperature phase transitions in single crystals of $Sr_xBa_{1-x}Nb_2O_6$ were continued. Time-of-flight neutron diffraction experiments were carried out on a crystal with x=0.70 in the temperature range between 293 K and 20 K. Diffraction pattern were taken along the [100], [001], [111], and [110] directions and partly studied under applied electrical field, too. The detected anomalies corroborate the existence of phase transitions at about 60 K and 198 K and give evidence of an additional one at about 230 K. Hysteresis effects, dependence on sample history, and relaxation of the structural changes indicate a non-equlibrium behaviour of the crystal.

Collaboration: Frank-Laboratory of Neutron Physics at JINR Dubna

W. Matz

Project Study for a Synchrotron Radiation Source at Rossendorf (ROSY)

The conceptual design report for a third generation synchrotron radiation source dedicated to materials research was prepared in a more detailed second version during this year. The first part, the scientific case, contains a compilation of potential users from the region including Poland and Czech Republic. The machine concept describes the layout of all main components of the storage ring.

supported by SMWK

Theory of Ion Beam Induced Processes in Solids

H.-U. Jäger

Modelling of transiently enhanced diffusion and of electrical activation of boron in crystalline silicon during post-implantation annealing:

The implantation-induced transient diffusion of boron and its electrical activation as a consequence of transitions onto substitutional sites is modelled by solving a system of coupled diffusion-reaction equations for the dopant and the silicon point defects (self-interstitials, vacancies). This approach has been extended. In order to describe the formation of very shallow p^+ layers where the boron peak concentration significantly exceeds the solid solubility limit, it has been taken into account that the transitions of boron atoms from clusters into solution affect directly the silicon point defect distributions.

supported by BMFT

Collaboration: Fraunhofer-Institute of Microelectronic Circuits and Systems, Dresden.

M. Posselt
*C. S. Murthy**

Channeling, dechanneling and damage accumulation in ion implantation into single-crystalline silicon:

For the first time, systematic investigations on channeling implantation of boron and phosphorus into the <100>, <110> and <111> axial channel directions at ion energies between 15 keV and 1 MeV and fluences between 10^{13} and 10^{16} cm^{-2} were performed. Using computer simulation program Crystal-TRIM, implantation profiles and channeling and dechanneling processes were studied under the influence of target temperature, an amorphous surface layer (e. g. native or screening oxide), pre-existing damage, and damage accumulation. It was shown that a simple model, assuming accumulation of vacancies and interstitials is sufficient to simulate the dependence of the shape of the range distributions on the fluence. A complete dechanneling already occurs at low defect concentrations. Therefore the nature of defects at higher concentrations is not relevant. In all cases considered the agreement between experimental range profiles and profiles calculated by Crystal-TRIM was good.

Collaboration: IBM Semiconductor R&D Center (*), East Fishkill; Institut für Integrierte Systeme der ETH Zürich; AT&T Bell Laboratories, Murray Hill; Hahn-Meitner-Institut, Berlin.

supported by BMFT

R. Mathar
M. Posselt

Effective charge theory for the electronic stopping of heavy ions in solids

The first step in the effective charge theory is the calculation of the ionization of an ion. The energy stripping criterion for the ionization degree was shown to offer some advantages compared to the velocity criterion. The second step is the transformation of the charge of the extended ion into an effective charge due to the linear dielectric response of the target material. On the basis of Kaneko's shell theory of electronic stopping in solid targets, the conditions were studied that allow the simple free electron gas model of the target still to be used.

supported by
BMFT

S. Reiß
K.-H. Heinig

Computer simulation of ion beam synthesis

The annealing stage of ion beam synthesis of buried oxide (SIMOX) and silicide layers has been studied. Of the sequence of processes (nucleation, growth, Ostwald ripening and coalescence), Ostwald ripening was modelled in detail. The initial condition for this process, the precipitate distribution, has been created by a crude model reproducing the experimentally observed precipitate distribution before Ostwald ripening. The computer simulation clearly shows that the Ostwald ripening tends to form a structure in the concentration profile of the implanted species. This self-organization process allows for the first time a consistent explanation of structures like "humps", "spikes" and "banding", which have been observed experimentally during ion beam synthesis of SIMOX layers.

Collaboration: CNRS Orsay; Kurchatov-Institute, Moscow.

supported by
BMFT, DAAD

M. Posselt
K.-H. Heinig

Comparison of BC and MD simulations for low-energy ion bombardment

Investigations on Si implantation into the <100> channel direction of single crystalline silicon at projectile energies of 250, 500 and 1000 eV were performed using two computer codes: (i) Crystal-TRIM which is based on the Binary Collision (BC) approximation and (ii) full Molecular Dynamics (MD) simulations. Identical repulsive potentials and identical implantation conditions were used. Implantation profiles and intersections of the trajectories of projectiles with lattice planes were considered. It was shown that at 1000 eV both codes yield similar kinematics of the projectiles and similar range profiles. The only difference is an overestimation of channeling by the BC code. This difference increases at 500 eV. At 250 eV, the kinematics and the range profiles obtained from BC and MD simulations become completely different. The results were used to estimate the range of

supported by
BMFT

validity of the BC approximation.

Collaboration: Institut für Festkörperphysik der FSU Jena.

K.-H. Heinig
*D. Stock**

Modification of Si surfaces by 225 eV Xe ion irradiation

The modification of vicinal Si(111) and Si(001)-(2x1) surfaces by 225 eV Xe ion irradiation has been studied using the same conditions as in a series of experiments carried out by Bedrossian, Picraux et al. at the Sandia National Labs. For the modelling the process has been separated in two stages: (i) Molecular Dynamics (MD) simulations of the ion impact and (ii) calculation of the step kinetics by reaction-diffusion equations. It is found that a single Xe ion impact produces surface vacancies arranged in one cluster, some adatoms, and on the average one sputtered atom. Contrary to explanations given in the literature so far, no mobile isolated vacancies are created which could control the step movement and/or the nucleation of depressions. We have shown, e. g. for adjacent terraces on a vicinal Si(001)-(2x1) surface separated by S_A- and S_B-steps, respectively, that the adatom diffusion as well as their attachment and detachment at steps and vacancy clusters determines the kinetics of the steps and results in the formation of double-height Si(001) steps.

supported by BMFT

Collaboration: Institut für Festkörperphysik der FSU Jena (*); AT&T Bell Laboratories, Murray Hill; Institute of Semiconductor Physics, Novosibirsk.

K.-H. Heinig

Molecular dynamics (MD) simulations of GRID-experiments

The MD method was applied to simulate γ-lineshapes of recoiling excited nuclei, which are measured by the γ-ray induced Doppler-broadening (GRID) method at the ILL Grenoble. The γ-lineshape contains information on the lifetime of the nuclear state, the initial lattice position of the recoiling atom as well as the interaction potential of the recoil with lattice atoms. Calculations for c-Si and c-Ti demonstrate that for experiments with monocrystalline samples strongly improved results can be expected.

supported by BMFT

Collaboration: Institute Laue-Langevin, Grenoble; University of Alicante.

Publications

Albrecht, J., Koch, B., Pham, M.T.,
Determination of an accurate depth distribution of sodium, calcium and aluminium in thin oxide layers using several methods,
Fresenius J. Anal. Chem. 346 (1993) 310

Barnitzke, W., Friedlein, R., Hentschel, R., Hiller, H., Schmidt-Böcking, H., Schneider, M., Stiebing, K., Streitz, H., Tyrroff, H., Wirth, H., Zippe, C., Zschornack, G.,
Status of the ECR ion source of the TU Dresden,
Proc. of the 11th Int. Workshop on Electron Cyclotron Resonance Ion Sources, May 1993, Groningen

Bischoff, L., Hesse, E., Hofmann, G., Naehring, F.K., Probst, W., Schmidt, B., Teichert, J.,
High current FIB system for micromechanics application,
Microel. Eng. 21 (1993) 197

Borany, J. von, Kögler, R.,
The influence of preamorphization on the properties of shallow p+n junctions in silicon radiation detectors,
Nucl. Instr. Meth. A 326 (1993) 42

Brauer, G., Eichhorn, F.,
Considerations about irradiation-induced precipitates in Soviet type reactor pressure vessel steels,
Nucl. Eng. & Design, 143 (1993) 301 - 307

Friedrich, L., Huttel, E., Hentschel, R., Tyrroff, H.,
A 7.25 GHz ECR ion source with floating disk operation,
Proc. of the 11th Int. Workshop on Electron Cyclotron Resonance Ion Sources, May 1993, Groningen (NL), KVI Report 996, (1993) 19

Grambole, D., Herrmann, F. and Hauffe, W.,
Large-depth profiling of hydrogen by line scans of the nuclear microbeam over slope planes cut with an ion beam,
Nucl. Instr. Meth. B 77 (1993) 117

Heera, V., Kögler, R., Skorupa, W., Grötzschel, R.,
Dose rate dependence of the ion beam induced epitaxial crystallization in silicon,
Nucl. Instr. Meth. B 80/81 (1993) 538

Heera, V., Kögler, R., Skorupa, W., Grötzschel, R.,
Dose rate dependence of the ion beam induced epitaxial crystallization in silicon,
Mat. Res. Soc. Symp. Proc. 279 (1993) 273

Heinitz, J., Ullemeyer, K., Walther, K.,
The possibility of neutron time-of-flight diffraction for investigation of the texture,
Proc. of Mtg. on advanced neutron spallation source, Vienna (Austria),
03./04.05.93, ed. Schuster, M., AUSTRON Planning Office, Vienna, p.99 - 102, July 1993

Hesse, E., Naehring, F.K.,
Narrow angle emission from a lithium liquid metal ion source,
J. Phys. D; Appl. Phys. 26 (1993) 717

Jäger, H.-U.,
An explanation of transient-enhanced diffusion and electrical activation of boron in crystalline silicon during postimplantation annealing,
Nucl. Instr. Meth. B 80/81 (1993) 679

Jäger, H.-U.,
Simulation of high-dose ion implantation-induced transient diffusion and of electrical activation of boron in crystalline silicon,
Simulation of Semiconductor Devices and Processes, vol. 5 Ed. by S. Selbherr, H. Stippel and E. Strasser, Springer Verlag Wien, 1993, 137

Kögler, R., Heera, V., Skorupa, W., Rück, D.,
Reduced reverse temperature of ion beam induced amorphization/crystallization for intermittent beam irradiation of Si,
Nucl. Instr. Meth. B 80/81 (1993) 556

Kolitsch, A., Hentschel, E., Richter, E.,
Wear reduction by ion implantation assisted deposition,
Vacuum 44 (1993) 291 - 295

Kolitsch, A., Hentschel, E., Richter, E.,
Depth profiles of C, N, and O on carbon coated steel surfaces made by IBAD,
Diamond and Related Materials 2 (1993) 1175 - 1178

Kolitsch, A., Hentschel, E., Richter, E.,
Depth profiles of C, N, and O on carbon coated steel surfaces,
Nucl. Instr. Meth. B 80/81 (1993) 258 - 261

Murthy, C. S., Posselt, M.,
Comparative study of simulated damage accumulation in silicon crystals,
Proc. of 3rd Int. Symp. on Process Physics and Modeling in Semiconductor Technology (183rd Meeting of the Electrochemical Soc.), Ed. by G.R. Srinivasan, K. Taniguchi and C.S. Murthy, The Electrochemical Soc., Pennington, NJ, Proc. vol. 93-6 (1993) 545

Neelmeijer, C. and Sobe, G.,
Hydrogen analysis in CrSiO thin films,
J. Radioanal. Nucl. Chem. Letters 175 (5) (1993) 389

Panknin, Dr., Wieser, E., Wollschläger, K., Skorupa, W., Grötzschel, R., Querner, G.,
Investigation of ion beam synthesized $FeSi_2$ and the α/β-phase transformation,
Vacuum 44, No. 3/4 (1993) 171

Panknin, D., Wieser, E., Skorupa, W., Vöhse, H., Albrecht, J.,
Formation of buried iron-cobalt silicide layers by high dose implantation,
Nucl. Instr. Meth. B 74 (1993) 213

Panknin, D., Wieser, E., Skorupa, W., Querner, G., Vöhse, H., Albrecht, J.,
Formation of buried ternary silicide layers in silicon by ion beam synthesis (IBS),
Mat. Res. Soc. Symp. Proc. 279 (1993) 111

Pham, M.T., Howitz, S., Hüller, J., et.al.,
Spectroscopic and electrochemical properties of ion-sensing membranes fabricated by ion implantation,
Sensors and Actuators B 13 - 14 (1993) 746

Posselt, M.,
Computer simulation of channeling implantation at high and medium energies,
Nucl. Instr. Meth. B 80/81 (1993) 28

Posselt, M.,
Computer simulation of channeling effects in ion implantation,
Proc. Symp. A (MRS Fall Meeting) "Beam Solid Interactions, Fundamentals & Applications", Ed. by M.A. Nastasi, N. Herbots, L.R. Harriott and R.S. Averback, MRS Symp. Proc., The Mat. Res. Soc., Pittsburgh, PA, vol. 279 (1993) 23

Reuther, H., Nikolov, O., Kruijer, S., Brand, R.A., Keune, W.,
High dose implantation of aluminium into iron,
Nucl. Instr. Meth. B 80/81 (1993) 348 - 351

Skorupa, W., Kögler, R., Schmalz, K., Gaworzewski, P., Morgenstern, G., Syhre, H.,
Iron gettering and doping in silicon due to MeV-Carbon-implantation,
Nucl. Instr. Meth. B 74 (1993) 70

Schmidt, B., Borany, J. von, Schubert, D.,
Application of wet chemical selective etch techniques to the fabrication of thin silicon detectors,
Nucl. Instr. Meth. A326 (1993) 21

Teichert, J., Tiunov, M.A.,
Achromatic two-stage E x B mass filter for a focused ion beam column with collimated beam,
Meas. Science Technology 4 (1993) 754

Teichert, J., Tiunov, M.A.,
Design of an achromatic man separator for a focused ion beam system,
Proc. SPIE "Charged Particle Optics" 2014 (1993) 85

Ullemeyer, K., Weber, K.,
Preferred orientations of phyllosilicates in mylonitic rocks and their implications for kinematic interpretation,
Fizika Zemli, 6, 104 (1993)

Wagner, W., Rauch, F., Feile, R., Ottermann, C.R. and Bange, K.,
Compaction of tungsten oxide films by ion-beam irradiation,
Thin Solid Films 235 (1993) 228 - 233

Walther, K., Isakov, N.N., Nikitin, A.N., Ullemeyer, K., Heinitz, J.,
Diffraction studies of textures in geomaterials using a high-resolution neutron spectrometer,
Fizika Zemli, 6, 37 (1993)

Walther, K., Kurtasov, S.F., Nikitin, A.N., Torina, E.G.,
Modeling deformation textures in high-temperature quartz,
Fizika Zemli, 6, 45 (1993)

Walther, K., Nikitin, A.N., Shermergor, T.D., Yakovlev, V.B.,
Determination of effective electroelastic constants of textured polycrystal rocks,
Fizika Zemli, 6, 83 (1993)

Wieser, E., Panknin, D., Grötzschel, R., Skorupa, W., Querner, G., Henrion, W., Albrecht, J.,
Ion beam synthesis of ternary ($Fe_{1-x}Co_x$)Si2,
Nucl. Instr. Meth. B 80/81 (1993) 867

Conference Contributions

Alefeld, B., Klimanek, P., Kulda, J., Lukaš, P., Mikula, P., Mücklich, A., Vrana, M., Wagner, V.,
Advanced neutron diffraction techniques for strain and stress measurements of polycrystalline materials,
EUROMAT 3, Paris (France), 08.-10. 06. 1993

Bischoff, L., Hesse, E., Panknin, D., Skorupa, W., Teichert, J.,
Writing implantation with a high current density focused ion beam,
Microcircuit Eng. '93, Maastricht (NL), Sept. 27 - 29, 1993

Böhm, G., Günzel, R.,
50 kV pulse generatro for plasma source ion implantation,
1st Int. Workshop on plasma-based ion implantation, Madison/Wisconsin (USA), Aug. 4 - 6, 1993

Eichhorn, F., Häußler, F., Baumbach, H.,
Structural studies on hydrating cement pastes,
9. International Conf. on Small-Angle Scattering, Saclay (France), 27.-30. 04. 1993

Eichhorn, F., Hempel, A.,
A DCD with a bent asymmetric crystal and a position sensitive detector,
Workshop on " Focusing Crystal Optics ", Physikalisch-Technische Bundesanstalt, Braunschweig, 10.-11. 05. 1993

Einfeld, D., Büttig, H., Dienel, S., Gläser, W., Goetz, Th., Guratzsch, H., Hartmann, B., Janssen, D., Krug, H., Linnemann, J., Matz, W., Murphy, J.B., Neumann, W., Oehme, W., Picard, M., Plesko, M., Pröhl, D., Schlenk, R., Tomassini, D., Tyrroff, H.,
The synchrotron light source ROSY,
3. European Conference on Accelerators in Applied Research and Technology, Orleans (France), 31. 08.-04. 09. 1993
Particle Accelerator Conference, Washington (USA), 17.-20. 05. 1993

Eremin, V., Ivanov, A., Strokan, N., Verbitskaya, E., Li, Z., Schmidt, B.,
Relaxation of radiation damages in silicon planar detectors,
1st Int. Conf. on Large Scale Applications and Radiation Hardness of Semiconductor Detectors, Florenz (Italy), July 1993

Eschner, Th., Klimanek, P., May, Ch., Mücklich, A.,
Simultaneous texture and grain size analysis by means of neutron diffraction,
ICOTOM 10, Clausthal - Zellerfeld , 20.-24. 09. 1993

Friedrich, M., Bürger, W., Grötzschel, R., Henke, D., Sun, G., Turuc, S., Hebert, D., Rothe, T., Stolz, W.,
Accelerator mass spectrometry at the Rossendorf tandem accelerators,
6th Int. Conf. on Accel. Mass Spectrometry, Canberra/Sydney (Australia), Sept. 27 - Oct. 1, 1993

Frischbutter, A., Helming, K., Heinitz, J., Voitus, W.,
Quartz fabric evolution within an orthogneiss fold - the case of fabric isotropization,
Workshop on "Textures of Geological Materials", Göttingen, Jan. 29 - 31, 1993

Frischbutter, A., Helming, K., Walther, K.,
Neutronographisch bestimmte Texturentwicklung der Quarzkomponente in einem Profil zunehmender Granatisierung,
Workshop on "Textures of Geological Materials", Göttingen, Jan. 29 - 31, 1993

Günzel, R., Wieser, E., Richter, E., Steffen, J.,
Plasma source ion implantation of oxygen and nitrogen in aluminium,
1st Int. Workshop on Plasma-based ion implantation, Madison/Wisconsin (USA), Aug. 4 - 6, 1993

Günzel, R., Wieser, E., Richter, E., Reuther, H.,
Plasma-immersion-implantation of oxygen and nitrogen into aluminium,
8th Int. Conf. on Surface Modification of Metals by Ion Beams, Kanazawa (Japan), Sept. 13 - 17, 1993

Häußler, F., Eichhorn, F., Baumbach, H.,
Description of the structural evolution of a hydrating portland cement paste by SANS,
Euroconference on " Neutrons in Surface Science and at Interfaces ", Studsvik (Sweden), 13.-17. 05. 1993

Häußler, F., Eichhorn, F., Birkholz, W., Baumbach, H.,
SANS studies in material sciences,
13. General Conference of the Condensed Matter Division of the European Physical Society, Regensburg, 29. 03.-02. 04. 1993

Heera, V., Kögler, R., Skorupa, W., Glaser, E.,
Ion beam induced epitaxial crystallization of 6HSiC,
3rd Europ. Conf. on Accel. in Appl. Res. and Technol., Orleans (France), Aug. 31 - Sept. 4, 1993

Heera, V., Kögler, R., Skorupa, W., Glaser, E.,
Ion beam induced epitaxial crystallization of single crystalline 6H-SiC,
Mat. Res. Soc. Fall Meeting, Boston (USA), Nov. 29 - Dec. 3, 1993

Heinig, K.-H., Stock, D., Zinovjev, V.A., Dvurechenskii, A.V., Aleksandrov, L.N.,
Formation of double-height Si(001) steps by sputtering with Xe ions - a computer simulation,
Symp. A, Mat. Res. Soc. Fall Meeting, Boston (USA), Nov. 29 - Dec. 3, 1993

Heinitz, J., Isakov, N.N., Nikitin, A.N., Suchoparov, A., Ullemeyer, W.,
Walther, K.,
Geplante Hochdruckexperimente am Neutronenstrahl des IBR-2,
Workshop " Textures of Geological Materials ", Göttingen, 27.-31. 01. 1993

Heinitz, J., Isakov, N.N., Nikitin, A.N., Suchoparov, A., Ullemeyer, W.,
Walther, K.,
A high-pressure device for in-situ measurements in a neutron beam,
ICOTOM 10, Clausthal - Zellerfeld, 20.-24. 09. 1993

Heinitz, J., Isakov, N.N., Nikitin, A.N., Suchoparov, A., Ullemeyer, W., Walther, K.,
Textur und Hochdruckexperimente: Möglichkeiten einer Hochdruckpresse im
Neutronenstrahl,
Workshop on "Textures of Geological Materials", Göttingen, Jan. 29 - 31, 1993

Hempel, A., Eichhorn, F., Häußler, F., Baumbach, H.,
A new version of a double-crystal diffractometer,
NATO Advanced Study Institute on " Modern Aspects of Small-Angle Scattering ", Como
(Italy), 12.-21. 05. 1993

Hempel, A., Hempel, M., Häußler, F., Eichhorn, F., Baumbach, H.,
Untersuchungen zur Strukturbildung bei der Hydration von Zement,
Arbeitstreffen 1993 des Verbundes " Forschung mit Neutronen ",
Benediktbeuren, 18.-20. 10. 1993

Hesse, E., Naehring, F.K.,
A lithium liquid metal ion source with a narrow angle emission for writing beam
lithography,
Microcircuit Eng. '93, Maastricht (NL), Sept. 27 - 29, 1993

Jäger, H.-U.,
Simulation of high-dose ion implantation-induced transient diffusion and of electrical
activation of boron in crystalline silicon,
5th Int. Conf. on Simulation of Semiconductor Devices and Processes, Vienna (Austria),
Sept. 7 - 9, 1993

Kämpf, H., Franzke, H.J., Betzl, M., Scheffzük, Ch.,
Texture investigation on halite and fluorite by neutron diffraction,
3. Conference on the Mechanical Behaviour of Salt, Palaiseau (France),
14.-16. 09. 1993

Klimanek, P., Kschidock, T., Lukaš, P., Mikula, P., Mücklich, A., Vrana, M.,
Substructure analysis in polycrystalline materials by means of neutron diffraction,
EUROMAT 3, Paris (France), 08.-10. 06. 1993

Kögler, R., Borany, J. von, Panknin, D., Skorupa, W.,
Electrical effects of residual defects in Si after high energy implantation of Ge+ ions and annealing,
3rd Europ. Conf. on Accel. in Appl. Res. and Technol., Orleans (France), Aug. 31 - Sept. 4, 1993

Kögler, R., Heera, V., Skorupa, W.,
Ion beam induced crystallization/amorphization in silicon at low temperature under pulsed ion beam,
Arbeitstreffen des BMFT-Verbundes "Festkörperphysik und Materialforschung mit nuklearen Methoden", Holzhau, Oct. 4 - 6, 1993

Kolitsch, A., Scheibe, H.-J., Ullmann, J., Weber, A.,
The effect of post-treatment of diamond-like carbon films with high energy ion beams,
Diamond Films '93, Albufeira (Portugal), Sept. 20 - 24, 1993

Kreißig, U., Grötzschel, R. and Behrisch, R.,
Simultaneous measurement of the hydrogen isotopes H, D., T. and ^{3}He with HIERD,
11th Int. Conf. on Ion Beam Analysis, Balatonfüred (Hungary), July 5 - 9, 1993

Kruijer, S., Nikolov, O., Reuther, H., Brand, R.A., Keune, W.,
A DCEMS study of Al-implanted α-^{57}Fe foils,
13th Gen. Conf. of the Condensed Matter Division of the Europ. Phys. Soc., Regensburg, March 29 - April 2, 1993

Kurtasov, S.F., Nikitin, A.N., Walther, K.,
Analysis of texture development in olivine rocks,
ICOTOM 10, Clausthal - Zellerfeld , 20.-24. 09. 1993

Matz, W., Einfeld, D.,
Vorschlag für eine Synchrotronstrahlungsquelle ROSY,
HASYLAB - Nutzertreffen, Hamburg, Jan. 28 - 29, 1993

Matz, W., Einfeld, D.,
Vorschlag für eine Synchrotronstrahlungsquelle ROSY,
31. Jahrestagung der Dt. Gesellschaft für Kristallographie, Bochum, March 10 - 12, 1993

Mücklich, A.,
Experimental errors in quantitative texture analysis from diffraction pole figures,
ICOTOM 10, Clausthal - Zellerfeld , 20.-24. 09. 1993, (eingeladen)

Murthy, C.S., Posselt, M.,
Comparative study of simulated damage accumulation in silicon crystals,
3rd Int. Symp. on Process Physics and Modeling in Semiconductro Technology, 183rd Meeting of The Electrochemical Soc., Honolulu (Hawaii), May 16 - 21, 1993

Nikolaev, D.I., Walther, K.,
Absorption correction for non-standard geometry for pole-figure measurements,
ICOTOM 10, Clausthal - Zellerfeld, 20.-24. 09. 1993

Panknin, D., Eichhorn, F., Wieser, E., Skorupa, W., Henrion, W., Albrecht, J.,
Electrical and optical properties of β-$FeSi_2$ after cobalt implantation and annealing,
Spring Meeting 1993 of the European Materials Research Society, Strasbourg (France),
04.-07. 05. 1993

Panknin, D., Henrion, W., Wieser, E., Voelskow, M., Skorupa, W., Vöhse, H.,
Electrical and optical properties of Co alloyed β-$FeSi_2$ formed by ion beam synthesis,
Mat. Res. Soc. Fall Meeting, Boston (USA), Nov. 29 - Dec. 3, 1993

Pham, M.T., Howitz, S.,
Fluidic microcell with sensor array in Si-glass technology,
7th Int. Conf. on Solid State Sensors and Actuators, Yokohama (Japan), June 1993

Pham, M.T., Howitz, S., Kunath, C., Kurth, E., Köhler, H.,
Rear side membrane structures for ISFET's applied in miniature analysis systems,
7th Int. Conf. EUROSENSORS, Budapest (Hungary), Sept. 1993

Posselt, M.,
Channeling effects and defect accumulation in ion implantation,
15th Int. Conf. on Atomic collisions in Solids (ICACS-15), London/Ontario (USA),
July 26 - 30, 1993

Posselt, M., Heinig, K.-H., Stock, D.,
Comparison of BC and MD simulations for low-energy ion bombardment of c-Si,
15th Int. Conf. on Atomic Collisions in Solids (ICACS-15), London/Ontario (USA),
July 26 - 30, 1993

Posselt, M.,
Computersimulation von Channeling, Dechanneling und der Defektakkumulation bei der
Ionenimplantation in einkristallines Silicium,
Treffen des Verbundes "Festkörperphysik und Materialforschung mit nuklearen Methoden",
Holzhau, Oct. 4 - 6, 1993

Prokert, F., Savenko, B.N.,
Studies of $Sr_xBa_{1-x}Nb_2O_6$ mixed crystals by neutron diffraction at temperatures between 15
K and 293 K,
31. Jahrestagung der Dt. Gesellschaft für Kristallographie, Bochum,
10.-12. 03. 1993

Prokert, F., Savenko, B.N.,
Thermal diffuse scattering in $Sr_xBa_{1-x}Nb_2O_6$,
Arbeitstreffen 1993 des Verbundes " Forschung mit Neutronen ",
Benediktbeuren, 18.-20. 10. 1993

Reiss, S., Heinig, K.-H., Skorupa, W., Weber, R.,
Experimental study and modeling of structure formation in buried layers at ion beam synthesis,
3rd Europ. Conf. on Accel. in Appl. Res. and Technol., Orleans (France), Aug. 31 - Sept. 4, 1993

Reiss, S., Heinig, K.-H., Weber, R., Skorupa, W.,
Is self-organisation during Ostwald Ripening a crucial process in ion beam synthesis?
Mat. Res. Soc. Fall Meeting, Boston (USA), Nov. 29 - Dec. 3, 1993

Reiss, S., Heinig, K.-H.,
Ostwald ripening during ion beam synthesis - a computer simulation for inhomogeneous systems,
E-MRS Spring Meeting, Strasbourg (France), May 4 - 7, 1993

Reiss, S., Heinig, K.-H.,
Structure formation during ion-beam synthesis - a computer simulation,
Treffen des Verbundes "Festkörperphysik und Materialforschung mit nuklearen Methoden", Holzhau, Oct. 4 - 6, 1993

Reuther, H., Nikolov, O., Kruijer, S., Brand, R.A., Keune, W., Liljequist, D., Weber, S., Scherrer, S.,
CEMS and DCEMS investigations of Al-implanted iron,
Int. Conf. on the Applications of the Mössbauer Effect, Vancouver (Canada), Aug. 8 - 13, 1993

Reuther, H.,
CEMS and AES investigations of Fe-Si-alloys produced by ion implantation,
5th Conf. on Applications of Surface and Interface Analysis, Catania (Italy), Oct. 4 - 8, 1993

Richter, E., Kolitsch, A.,
Ionenstrahltechniken - neue Möglichkeiten zur gezielten Modifizierung von Werkstoffoberflächen,
Tagung Oberflächenanalytik, Chemnitz, June 16 - 19, 1993

Richter, E., Chudoba, Th.,
Implantation of oxygen and nitrogen into magnesium,
8th Int. Conf. on Surface Modification of Metals by Ion Beams, Kanazawa (Japan), Sept. 13 - 17, 1993

Richter, E.,
Verbesserungen von Werkstoffen durch Ionenstrahltechnik,
Werkstofftag '93, München, March 1993

Scheffzük, Ch., Kämpf, H., Betzl, M.,
Texture investigation on natural halite by neutron diffraction,
Arbeitstreffen 1993 des Verbundes " Forschung mit Neutronen ", Benediktbeuren, 18.-20. 10. 1993

Schmidt, B.,
Electrochemical etch stop behaviour on ion implanted silicon pn-junctions,
Micro System Technologies (MST) Russia, St. Petersburg (Russia), June 1993

Schmidt, B., Borany, J. von, Todt, U., Erlebach, A.,
Preparation and characterization of ultrathin crystalline silicon membranes,
7th Int. Conf. EUROSENSORS, Budapest (Hungary), Sept. 1993

Skrotzki, W., Dornbusch, J., Heinicke, F., Ullemeyer, K.,
Formation of oblique shape and lattice preferred orientation in a quartz band of a gneissic mylonite,
ICOTOM 10, Clausthal - Zellerfeld, 20.-24. 09. 1993

Teichert, J., Tinnov, M.A.,
Design of an achromatic mass separator for a focused ion beam system,
Int. Symp. on Optical Appl. Sc. and Eng., SPIE '93, San Diego (USA), July 11 - 16, 1993

Teichert, J., Bischoff, L., Hesse, E., Panknin, D., Skorupa, W.,
Formation of CoSi2 wires by maskless implantation with the focused ion beam,
Mat. Res. Soc. Fall Meeting, Boston (USA), Nov. 29 - Dec. 3, 1993

Ullemeyer, K., Heinitz, J., Walther, K.,
Neutron diffraction measurements on geological samples at NSHR,
Workshop "Neutron Texture Analysis", Geesthacht, Sept. 27 - 29, 1993

Wagner, W., Rauch, F. and Bange, K.,
Stoichiometry of NiO_xHy films determined by ion-beam analysis,
ECCART, Orleans (France), Oct. 1993

Wagner, W. and Bange, K.,
Stoichiometry of uncoated and coated glass surfaces,
DGG Glasforum, Würzburg, March 1993

Walther, K.,
Investigation of the texture of geological samples by means of high resolution time-of-flight diffraction,
International Workshop on Neutronography and Radiation Physics of Solids, Jekatarinburg (Russia), 18.-23. 03. 1993

Walther, K.,
Probleme der Indexierung von Diffraktogrammen niedersymmetrischer geologischer Proben,
Workshop " Textures of Geological Materials ", Göttingen, 27.-31. 01. 1993

Walther, K., Heinitz, J., Ullemeyer, K.,
Texture investigation by means of the time of flight method,
Workshop "Neutron Texture Analysis", Geesthacht, Sept. 27 - 29, 1993

Weber, R., Skorupa, W.,
Precipitation studies in oxygen- and nitrogen rich silicon formed by high dose implantation,
Spring Meeting 1993 of the European Mat. Res. Soc., Symp. G, Strasbourg (France), May 4 - 7, 1993

Weber, R., Skorupa, W.,
Experimentelle Untersuchungen zum Ostwaldreifen in sauerstoffimplantiertem Silizium, Arbeitstreffen des BMFT-Verbundes "Festkörperphysik und Materialforschung mit nuklearen Methoden", Holzhau, Oct. 4 - 6, 1993

Weber, R., Yankov, R., Müller, R., Skorupa, W., Reiss, S., Heinig, K.-H.,
Experimental study of precipitation processes in oxygen implanted silicon,
Mat.Res. Soc. Fall Meeting, Boston (USA), Nov. 29 - Dec. 3, 1993

Weber, R., Müller, R., Skorupa, W., Reiss, S., Heinig, K.-H.,
Precipitation studies for modeling high dose oxygen- and nitrogen implantation,
Symp. A (Mat. synth. and proc. using ion beams), MRS Fall Meeting, Boston (USA), Nov. 29 - Dec. 3, 1993

Zinovjev, V.A., Aleksandrov, L.N., Dvurechenskii, A.V., Heinig, K.-H., Stock, D.,
Modeling of Si deposition and sputtering at Si (111) surfaces under irradiation with low-energy ions,
Spring Meeting 1993 of the European Mat. Res. Soc., Strasbourg (France), May 4 - 7, 1993

Seminars

Borany, J. von,
Properties of implanted n+-layers in HP-Ge substrates for EUROBALL-stack detectors,
CRN Strasbourg (France), June 1993

Eichhorn, F.,
Experimente zur Neutronenoptik perfekter Kristalle,
Seminarvortrag, Universität Osnabrück, Fachbereich Physik, 01. 07. 1993

Fiehn, H.,
Inhalt und Zielstellungen des FIM-Projektes,
1. Workshop Mikrosystemtechnik Sachsen, FhG-IMS2 Dresden, May 1993

Grambole, D.,
Untersuchung von Wasserstoff- und Deuteriumprofilen bis zu 10 μm Tiefe mittels Kernmikrosonde und Ionenstrahl-Böschunsschnitt-Verfahren,
J.-W.-Goethe-Universität Frankfurt/M., Inst. f. Kernphysik, 20.01.1993

Grambole, D.,
Kernmikrosonde für Elementanalyse - Grundlagen und Anwendungen,
TU Dresden, Abt. Physik, Inst. f. Oberflächen- u. Mikrostrukturphysik, 14.04.1993

Heinig, K.-H.,
Molekulardynamische Simulationen von GRID-Experimenten,
FSU Jena, Fakultät für Physik und Astronomie, Febr. 26, 1993

Heinig, K.-H.,
Molecular dynamics simulation of the slowing down of low-energy ions in Si - application to different phenomena,
Inst. of Semiconductor Physics, Novosibirsk (Russia), April 4, 1993

Heinig, K.-H.,
Interaction of low-energy ions with silicon: molecular dynamics simulations,
Seminarvortrag AT & T Bell Labs., Murray Hill (USA), Dec. 8, 1993

Hüller, J., Howitz, S., Pham, M.T.,
Entwicklung schwermtallionensensitiver ISFET-Membranen mittels Ionenstrahlsynthese und deren Integration in ein Fluidik-ISFET-Mikrosystem,
Forschungsgesellschaft für Meß- und Sensortechnik, Berlin, Febr. 1993

Hüller, J., Pham, M.T., Hoffmann, W., Howitz, S.,
Entwicklung neuer Membranmaterialien für ionensensitive Feldeffekttransistoren,
Forschungsgesellschaft für Meß- und Sensortechnik, 1. Dresdner Sensor-Symposium, Dresden, Dec. 1993

Howitz, S., Pham, M.T., Bürger, M., Fiehn, H., Hellfeld, T., Kunath, C., Wolf, H.,
Integriertes Fluidik-ISFET-Mikrosystem,
Statusseminar, FZ Rossendorf, Oct. 1993

Jäger, H.-U.,
Punktdefektgestützte Diffusion im TESIM4,
FhG-IMS2, Dresden, Febr. 4, 1993

Jäger, H.-U.,
Punktdefektgestützte Dotantendiffusion im Silicium,
Institut für Halbleiterphysik, Frankfurt/O., June 15, 1993

Posselt, M.,
Computer simulation of channeling effects in ion implantation,
ETH Zürich, Inst. f. Integrierte Systeme, June 11, 1993

Schmidt, B.,
Herstellungsmöglichkeiten für ultradünne Silicium-Membranen,
1. Workshop Mikrosystemtechnik Sachsen, FhG-IMS2 Dresden, May 1993

Skorupa, W.,
Erzeugung und Eigenschaften von SiO2- und Si3N4-Oberflächenschichten durch Hochdosisimplantation,
Universität Frankfurt/M., Fakultäten f. Angewandte Physik u. Kernphysik, 26.1.1993

Skorupa, W.,
Ion beam modification of semiconductors - Activities at Research Center Rossendorf,
Argonne Nat. Lab., Mat. Sc. Div., 06.12.1993

Skorupa, W.,
CIRIT-Special Course "Characterization of Materials in Microelectronics",
Barcelona, Spain, 20./21.12.1993

Steffen, J.,
Analyse chemischer Bindungszustände mit der Valenzband-Augerelektronenspektroskopie,
Universität Hohenheim, Institut für Physik, Stuttgart, 07.06.1993

Steffen, J.,
Strategische Grundlagenforschung in Japan auf dem Gebiet Neue Materialien mittels Ionenstrahlen,
Japan-Info Veranstaltung d. VDI-Technologiezentrums, Düsseldorf, 12.11.1993

Walther, K.,
Probleme bei der neutronographischen Bestimmung des dreidimensionalen Spannungszustandes,
GeoForschungszentrum Potsdam, 28.10.93

Reports

Einfeld, D., Krüssel, A., Tyrroff, H.,
Kapitel 6 MAGNETE in:
ROSY, Rossendorfer Synchrotronstrahlungsquelle, Projektvorschlag 2. Fassung,
FZR 93-27, Nov. 1993, II 83-116

Einfeld, D., Matz, W.,
ROSY - Rossendorfer Synchrotronstrahlungsquelle, Projektvorschlag 2. Fassung,
FZR 93-27, Nov. 1993

Häußler, F., Eichhorn, F., Birkholz, W., Baumbach, H.,
SANS study of hardening cement pastes and solid state nuclear track detectors,
Proc. of Int. Sem. on Structural Investigations on Pulsed Neutron Sources,
Dubna, Sept. 1 - 4, 1993, JINR E3-93-65, 1993

Matz, W., (ed.)
Workshop on a project for a FZR - beam line at ESRF,
FZR 93-24, Oct. 1993

Prokert, F., Savenko, B.N., Balagurov, A.M.,
Accurate determination of IC modulation parameter in $Sr_xBa_{1-x}Nb_2O_6$ from second order satellites of neutron diffraction TOF spectra,
Communications JINR, E14-93-276, Dubna 1993

Wagenaar, E.,
Beschreibung der Software zur Gewinnung und Bearbeitung von Bilddaten der Mikrostrahlanlage IMSA-100,
FZR-report 93-17, Juli 1993, Rossendorf

Arbeitstreffen Nutzung einer zukünftigen Synchrotronstrahlungsquelle Dresden,
15. und 16. 12. 1992, Sammlung der Beiträge, Herausgeber: Matz, W.,
FZR 93 - 03, Rossendorf, Januar 1993

Patents

Teichert, J., Hesse, E.,
Flüssigmetall-Ionenquelle zur Erzeugung von Kobalt-Ionenstrahlen,
Aktenzeichen P 4 312 028.8
eingereicht 13.04.1993

Heinig, K.-H., Reiss, S., Schmidt, B., Skorupa, W.,
Verfahren zur Herstellung faden- und/oder röhrenförmiger Mikrostrukturen in Festkörpern,
Aktenzeichen P 4 315 329
Erfindungsmeldung 1108 vom 5.10.1993

Howitz, S., Pham, M.T.,
Verfahren zur Herstellung eines ISFET mit Rückseitenmembran,
Aktenzeichen P 4316086.7
angemeldet am 13.05.93

Howitz, S., Pham, M.T.,
Mikrokapillare mit integrierten chemischen Mikrosensoren und Verfahren zu ihrer Herstellung,
Aktenzeichen P 4318407.3
angemeldet am 03.06.1993

Pham, M.T., Howitz, S.,
Redundanz-ISFET,
Aktenzeichen P 4316003.4
angemeldet am 13.05.1993

Laboratory Visits

Bischoff, L., Teichert, J.,
Rutherford Appleton Laboratory, Didcot (GB),
Nov. 1 - 7, 1993

Boede, W., Reichel, P.,
VIK Dubna (Russia),
Jan. 5 - Febr. 2, 1993

Heinig, K.-H.,
At & T Bell Laboratories, Murray Hill, NJ (U.S.A),
Dec. 3 - 8, 1993

Mücklich, A.,
UJF Řež (ČSFR),
3 weeks

Neelmeijer, Ch., Wagner, W.,
Louvre, Paris (France),
Nov. 21 - Dec. 4, 1993

Posselt, M.,
IBM Semiconductor R & D Center, East Fishkill Facility,
Hopewell Junction, NY (U.S.A.),
July 20 - 24, 1993

Reichel, P., Walther, K.,
UJF Řež (ČSFR),
1 week

Schmidt, B.,
Physikalisch-Technisches Joffé-Institut, St. Petersburg (Russia),
June 14 - 26, 1993

Walther, K.,
VIK Dubna (Russia),
8 weeks

Departments of the Institute

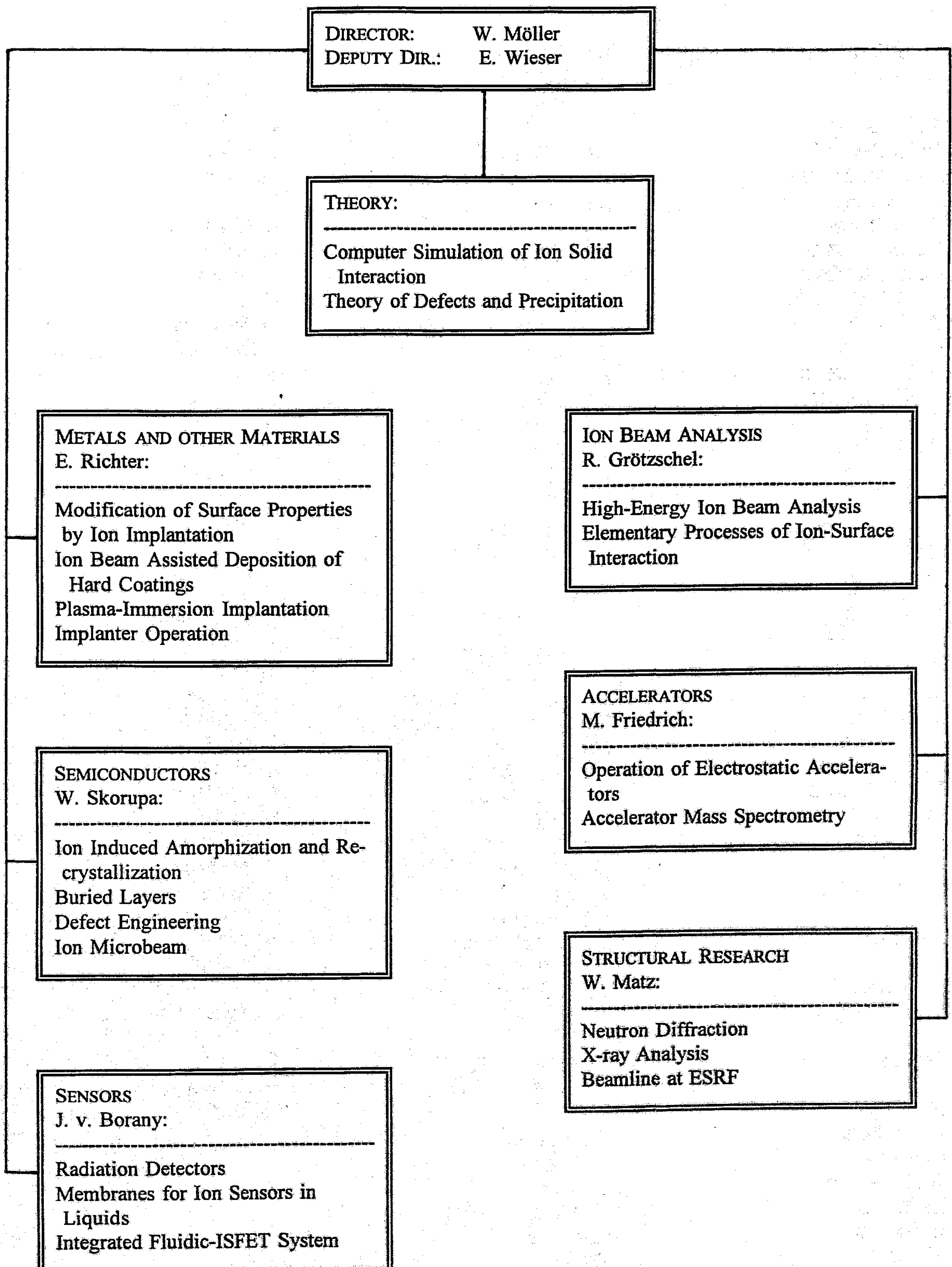

List of Personnel

Director: Prof. W. Möller

Deputy Director: Prof. E. Wieser

Scientific Staff:

Permanent:

Dr. M. Betzl
Dr. L. Bischoff
Dr. J. von Borany
Dr. W. Bürger
Dr. F. Eichhorn
Dr. M. Friedrich
Dr. D. Grambole
Dr. R. Grötzschel
Dr. R. Günzel
Dr. V. Heera
Dr. K.-H. Heinig
Dr. H.-U. Jäger
Dr. A. Kolitsch
Dr. R. Kögler
Dr. U. Kreißig
Dr. W. Matz
Dr. A. Mücklich
Dr. C. Neelmeijer
Dr. D. Panknin
Dr. M.T. Pham
Dr. M. Posselt
Dr. F. Prokert
Dr. H. Reuther
Dr. E. Richter
Dr. B. Schmidt
Dr. J. Schöneich
Dr. H. Seifarth
Dr. W. Skorupa
Dr. J. Steffen
Dr. J. Teichert
Dr. H. Tyrroff
Dr. M. Voelskow
Dr. M. Seidel
Dr. A. Steinbach
T. Vopel
Dr. W. Wagner
Dr. K. Walther

Post Docs:

Dr. J. Brutscher
Dr. H. Weishart

Projects:

M. Bürger
Dr. H. Fiehn
D. Henke
Dr. S. Howitz
Dr. J. Hüller
R. Küchler
M. Mäder
Prof. I. Sandner

PhD Students:

T. Chudoba
J. Goerigk
N. Hatzopoulos
A. Hempel
T. Henkel
E. Hesse
W. Jiang
R. Mathar
D. Möller
U. Müller
G. Sun
S. Reiß
R. Weber

Guests:

Dr. Aoki
Dr. D. Danailov
Dr. A.A. Deshkowskaja
Prof. A. V. Dvurechenskii
Dr. V. Eremin
Prof. F. Fujimoto
Dr. V. Konoplev
M. Mařik
Prof. K. Nomura
Dr. V. Petuchov
J. Rozinek
B.N. Savenko
Dr. E. Verbitskaya
Dr. R. Yankov
Dr. V. Zinovyev

Technical Staff:

Permanent:

J. Altmann
R. Aniol
I. Beatus
W. Boede
K.-D. Butter
W. Gäßner
B. Gebauer
H.-J. Grahl
P. Hartmann
F. Herrmann
G. Hofmann
R. Hüller
M. Iseke
S. Klare
R. Kliemann
L. Kumpf
G. Küster
D. Maul
M. Mißbach
I. Morawitz
K. Müller
F. Nötzold
W. Probst
A. Protze
E. Quaritsch
P. Reichel
B. Richter
M. Roch
E. Rost
C. Rußig
B. Scheumann
H. Schluttig
E. Schmidt
G. Schnabel
J. Schneider
A. Scholz
J. Schröter
C. Schulenberg
H. Seifert
U. Strauch
K. Thiemig
S. Turuc
A. Vetter
A. Weise
I. Winkler

Projects:

G. Franz
H. Hempel
H. Thümer